

# Dynamic Simulations Help Improve Generator Protection

Ramón Sandoval

*Comisión Federal de Electricidad*

Armando Guzmán and Héctor J. Altuve

*Schweitzer Engineering Laboratories, Inc.*

Published in

*Synchronous Generator Protection and Control: A Collection of  
Technical Papers Representing Modern Solutions, 2019*

Previously presented at the

6th Annual Clemson University Power Systems Conference, March 2007

Originally presented at the

33rd Annual Western Protective Relay Conference, October 2006

# Dynamic Simulations Help Improve Generator Protection

Ramón Sandoval, *Comisión Federal de Electricidad*  
Armando Guzmán and Héctor J. Altuve, *Schweitzer Engineering Laboratories, Inc.*

**Abstract**—This paper describes a digital simulation study of a set of two 160 MW generating units operating in the Juan de Dios Bádiz Paredes thermal power station, in Topolobampo, Sinaloa, Mexico. This plant belongs to Comisión Federal de Electricidad, the national Mexican utility. We first discuss the factors that limit the active and reactive power delivered by a generating unit, such as thermal and voltage limits, power-system imposed limits, and the minimum excitation limiter. We then describe generator protection functions related to the capability curve. Later, we propose a P-Q plane-based scheme that provides generator loss-of-field protection and capability-curve violation alarming. Finally, we present the simulation results of loss-of-field and loss-of-synchronism conditions of one of the two generating units for several cases, including different initial load conditions, different loss-of-field modes, and different numbers of units on line.

## I. INTRODUCTION

Power-generating plants represent approximately 50 percent of the capital investment in an electric power system. Generator outages caused by faults, abnormal operating conditions, or even generator protection misoperation are very costly when they occur. Synchronous generators are exposed to more harmful operating conditions than any other power system element. A complete generator protection system must include a variety of protection functions to respond to the different possible abnormal operating conditions.

Modern generator-protection relays include virtually all the required protection functions. Multifunction relays can provide even small-capacity generators with complete protection at low cost. However, selecting the protection functions that a particular generator needs and determining appropriate setting values require a thorough knowledge of the protected machine. Therefore, dynamic digital simulation using available computer programs is a highly recommended tool for protection engineers.

This paper describes a digital simulation study of a set of two 160 MW generating units operating in the Juan de Dios Bádiz Paredes thermal power station, in Topolobampo, Sinaloa, Mexico. The plant belongs to Comisión Federal de Electricidad, the national Mexican utility. These generators are interconnected with two substations of the national Mexican power system through two 230 kV transmission lines. The simulation includes the generators and their control systems, the step-up transformers, the transmission lines, and an equivalent of the power system beyond the area of interest. Generator models include speed and voltage regulators and power system stabilizers. These models were validated using the results of factory and commissioning tests of both units.

After discussing the factors limiting the output of generating units, the paper describes traditional protection functions related to the capability curve, such as stator thermal, rotor thermal, motoring, overvoltage, undervoltage, and loss-of-field protection. The paper proposes P-Q plane-based loss-of-field protection and capability-curve violation alarming functions. The simulation results for several cases of generator loss-of-excitation and loss-of-synchronism conditions illustrate the impact of initial load, loss-of-field mode, and number of generator units on line. Simulation results for each case include graphics showing the behavior of power, voltage, and current as functions of time and also the resulting trajectory in the impedance plane. Introducing the time variable, we present the simulation results in the three-dimension resistance-reactance-time space. Finally, a P-Q plane representation completes the set of graphic tools for analyzing the generator, power system, and protection behavior.

## II. FACTORS LIMITING THE ACTIVE AND REACTIVE POWER DELIVERED BY A GENERATING UNIT

A power system must continuously meet the variable demand for active and reactive electric power. To meet this requirement, the system should have enough reserve of active and reactive power and the capability to control active and reactive power at all times.

Active- and reactive-power flows in a power system are relatively independent. For a transmission line connecting two sources, active-power flow depends mainly on the angle between the voltages at the line terminals. Active power flows from the leading-voltage line end to the lagging-voltage line end. On the other hand, reactive-power transfer depends mainly on the voltage magnitudes. Reactive power flows from the line terminal having higher voltage magnitude to the line terminal with lower voltage magnitude.

Power-system operating frequency strongly depends on the active-power balance. Therefore, active-power control is closely related to frequency control. Power-system operating voltage magnitudes depend mainly on reactive-power balance. As a consequence, there is a close relationship between reactive-power control and voltage control in the power system.

Synchronous generators have the capability of generating active power and of generating (overexcited generator) or absorbing (underexcited generator) reactive power.

Speed turbine governors of generating units provide primary local control of active-power generation at generating plants. Additionally, automatic generation control (AGC),

performed by control center computers, processes real-time, system-level information and sends remote control commands to a number of generating units located in the control area. Automatic voltage regulators (AVRs) provide generator-voltage control. An AVR is a closed-loop control system that compares the generator terminal voltage to a reference set point and adjusts the excitation to keep the voltage within an operation band.

Several factors limit the active and reactive power that a generating unit can deliver to the power system under given operating conditions. These factors include the generator capability curve (determined by the machine design), voltage limits, power-system stability limits, the minimum excitation limiter (MEL), and the overexcitation limiter (OEL).

### A. Generator Capability Curve

Synchronous generators are rated in terms of the maximum MVA output that they can carry continuously without overheating, at a specified voltage and power factor. Generator capability curves provided by the manufacturer represent the machine thermal limits in a P-Q plane at nominal voltage (see Fig. 1).

#### 1) Active- and Reactive-Power Limits

The active-power output is limited by the prime mover capability to a value within the MVA rating. The driving torque available for the turbine imposes this limit. The turbine is usually sized to deliver rated MW at rated power factor. The vertical line through point B of Fig. 1 represents the typical generator active-power limit. However, there are cases in which the turbine is rated below this value.

The continuous reactive-power output capability is limited by three factors: armature-current limit, field-current limit, and stator-end region heating limit.

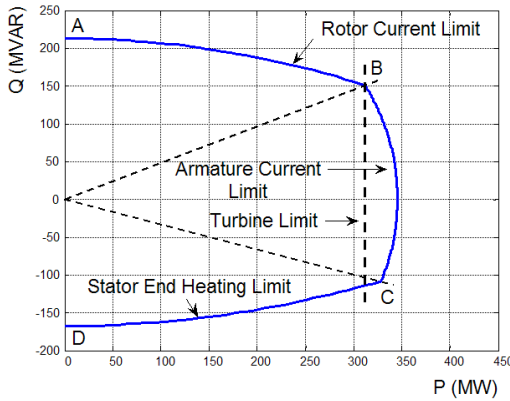


Fig. 1 Generator capability curve

#### a) Armature-Current Limit

The armature-current limit results from the stator copper power losses. There is a maximum current that the generator armature can carry continuously without exceeding the allowable operating temperature. In the P-Q plane the armature-current limit defines a circle with center at the origin. At rated voltage, the circle radius equals the generator MVA rating (curve BC in Fig. 1):

$$\text{Center } (P, Q) = 0, 0 \quad (1)$$

$$\text{Radius} = \text{Rated MVA} \quad (2)$$

#### b) Rotor-Current Limit

Copper power losses in the rotor winding impose a limit to the generator field current. The relationship between the active and reactive powers for a given field current is a circle (curve AB in Fig. 1) centered at the negative part of the Q-axis [1] [2].

Fig. 2 depicts a generator connected to a power system. The generator internal voltage and synchronous reactance are  $E_q$  and  $X_d$ , respectively. The generator terminal voltage is  $V_t$ . The generator model assumes constant field current and neglects saliency effects and stator resistance. Neglecting saliency effects means assuming the direct-axis reactance  $X_d$  to be equal to the quadrature-axis reactance  $X_q$ . The power system voltage and reactance are  $E_s$  and  $X_s$ , respectively.  $X_s$  includes the reactances of the step-up transformer and the equivalent power system. For this configuration the center position and radius of the rotor-current limit circle are:

$$\text{Center } (P, Q) = 0, -\frac{V_t^2}{X_d} \quad (3)$$

$$\text{Radius} = \frac{E_q \cdot V_t}{X_d} \quad (4)$$

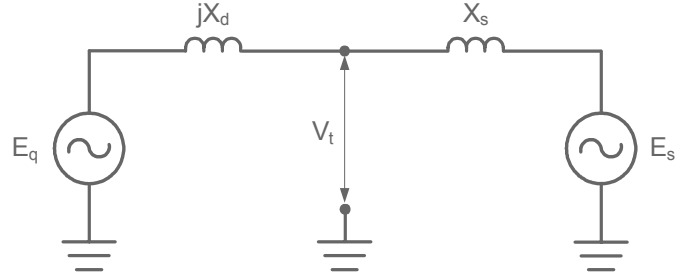


Fig. 2 Simple power-system diagram

The circles representing the rotor-current limit and the armature-current limit intersect at a point (point B in Fig. 1), which represents the machine nameplate MVA and power factor rating.

#### c) Stator-end region heating limit

The armature end region heating imposes a third operational limit to the generator in the underexcited region (curve CD in Fig. 1). The main generator magnetic flux is a radial flux, parallel to the stator laminations. However, the armature end-turn leakage flux is an axial flux, perpendicular to the stator laminations. The resulting eddy currents in the laminations produce localized heating in the end region.

When the generator operates in an overexcited condition, the field current is high and the retaining ring is saturated by the resulting high magnetic flux. The high reluctance of the retaining ring keeps end leakage flux in a low value. On the other hand, for underexcited generator operation, the field current is low, the retaining ring is not saturated, and the leakage flux is high. Furthermore, in the underexcited generator condition, the flux produced by the armature currents adds to

the flux produced by the field current; as a result, the end turn flux enhances the axial flux in the end region. The resulting heating effect in the armature end region limits the generator output, particularly in a round-rotor machine [3] [4].

Reference [4] shows that the stator end heating limit of the capability curve (curve CD in Fig. 1) is a circle centered at the positive part of the Q-axis, under the assumption that the end core leakage flux is proportional to the main air gap flux and that the thermal energy produced by eddy currents is proportional to the square of the end region magnetic flux.

According to [4], the center position and radius of the stator-end heating limit circle are:

$$\text{Center (P,Q)} = 0, K_1 \frac{V_t^2}{X_d} \quad (5)$$

$$\text{Radius} = K_2 \cdot \frac{V_t}{X_d} \quad (6)$$

Where:

$$K_1 = -\frac{N_a N_f - N_f^2}{N_f^2 + N_f^2 - 2 N_a N_f} \quad (7)$$

$$K_2 = \sqrt{\frac{\Delta\theta}{K_t (N_f^2 + N_a^2 - 2 N_a N_f)}} \quad (8)$$

$N_f$  and  $N_a$  are the number of turns of the field and armature windings, respectively;  $\Delta\theta$  is the maximum permissible continuous temperature rise above the no-load temperature in the end core region;  $K_t$  is a proportionality constant relating the thermal energy with the square of the end region magnetic flux.

Actual generator capability curves may not comply with (7) and (8). For example, the stator-end heating limit of the Juan de Dios Batiz Paredes power station generators (Fig. 3) is a circle centered at the point (54.8 MW, 139.9 MVAR), with a radius of 244 MVA. On the other hand, the actual capability curve depicted in Fig. 5 does comply with (7) and (8). The circle is centered at the point (0 MW, 750.2 MVAR), and its radius equals 918.2 MVA.

## 2) Effect of Voltage and Coolant Pressure

From the previous analysis it is clear that the circles representing the three generator thermal limits in the capability curve depend on the armature voltage. Manufacturers typically provide generator capability curves at nominal voltage. Using (1) through (6) we may derive the capability curve for other voltage values.

Generator power output capability also depends on the effectiveness of the cooling system. In hydrogen-cooled generators, for example, the capability is a function of hydrogen pressure. Fig. 3 shows the capability curve at nominal voltage of a 160 MW hydrogen-cooled steam turbine-driven generator at rated armature voltage (the Juan de Dios Batiz Paredes thermal power station generator). The capability curve is really a family of curves with the coolant pressure as a parameter. The dotted straight lines in the figure are the loci of constant power factor.

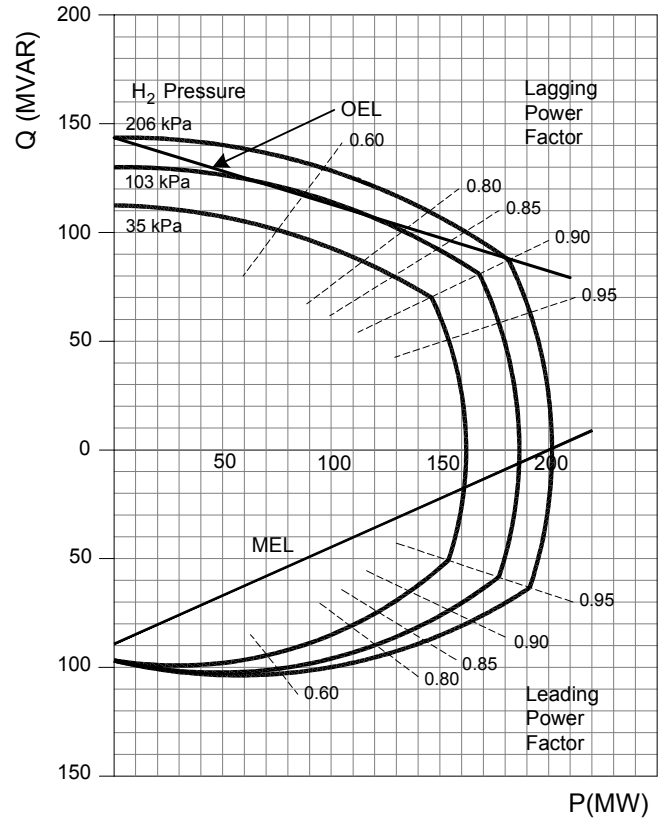


Fig. 3 Capability curve at nominal voltage of a 160 MW, 202 MVA, 15 kV, 0.9 PF, 3600 RPM, 60 Hz, hydrogen-cooled steam-turbine generator

## B. Voltage Limits

The generator terminal voltage is restricted to an operating band determined either by the generator or the step-up transformer operating voltage limits. The permissible operating range of cylindrical-rotor [5] or salient pole generators [6] is  $\pm 5$  percent rated voltage, at rated kVA, frequency and power factor. Transformers should meet two voltage requirements for any primary or secondary tap position. The transformer should be capable of operating at 110 percent rated voltage with no load. The primary winding should also be capable of operating continuously at the voltage required to produce 105 percent rated voltage at the secondary terminals with rated transformer load at 0.8 power factor.

## C. Steady-State Stability Limit (SSSL)

Another limit to the power delivered by the generating unit is system stability. Power systems normally operate close to the nominal frequency. All synchronous machines connected to the power system operate at the same average speed. The generator speed governors maintain the machine speed close to its nominal value. There is a balance between generated and consumed active power under normal power system operating conditions.

Random changes in load and system configuration constantly take place and impose small disturbances to the power system. The property of a power system to keep the normal operating condition under these small slow changes of system loading is what we call steady-state stability or system stability for small perturbations.

For the two-machine power system depicted in Fig. 2, the active-power transfer  $P_e$  is given by:

$$P_e = \frac{E_q E_s}{X_d + X_s} \sin \delta \quad (9)$$

Where the system power angle  $\delta$  is the angle between  $E_q$  and  $E_s$ . Fig. 4 depicts three power-angle curves, which are plots of (9) for different values of the internal generator voltage  $E_q$  ( $E_{q0} > E_{q1} > E_{q2}$ ). The dashed horizontal line represents the mechanical power  $P_m$  provided by the prime mover to the generator. This ideal lossless system operates at the point where the mechanical power input to the generator equals the electrical power delivered to the system ( $P_m = P_e$ ). Hence, the value of angle  $\delta$  corresponds to the intersection of the  $P_m$  straight line with the power angle curve.

We may increase the load in small steps ( $P_m$  increases) until we reach the tip of the power curve. The system remains stable until the power angle  $\delta = 90^\circ$ . Beyond the curve maximum ( $\delta > 90^\circ$ ) a load increase causes a decrease in the transfer power and the system loses synchronism. The value of  $P_e$  for  $\delta = 90^\circ$  represents the SSSL for this ideal lossless system. This is the maximum power that the electrical system can transfer.

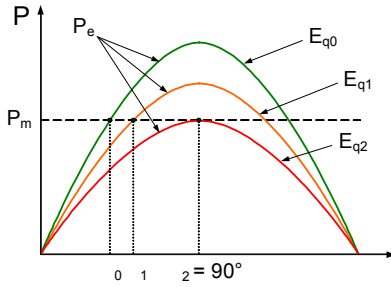


Fig. 4 Power-angle curves for different generator excitation levels

The power system may also lose synchronism for a fixed value of mechanical power if the generator internal voltage  $E_q$  is reduced. This loss-of-synchronism could occur if the operator reduces generator excitation to absorb reactive power from the system. Fig. 4 shows the effect of reducing the internal voltage from an initial value  $E_{q0}$  to a lower value  $E_{q2}$ : the power angle increases from  $\delta_0$  to  $90^\circ$ , and the system reaches the SSSL. Any further decrease of the internal voltage makes the system unstable.

It has been shown [1] [7] that, for the ideal lossless system depicted in Fig. 2, the system SSSL plots in the P-Q plane as a circle centered at the positive part of the Q-axis. The center position and radius of the SSSL circle are:

$$\text{Center (P, Q)} = 0, \frac{V_t^2}{2} \left( \frac{1}{X_s} - \frac{1}{X_d} \right) \quad (10)$$

$$\text{Radius} = \frac{V_t^2}{2} \left( \frac{1}{X_d} + \frac{1}{X_s} \right) \quad (11)$$

The previous analysis is valid for the case of manual voltage regulator operation. In this case, the generator excitation remains fixed for each power angle curve in Fig. 4. Hence,

(10) and (11) describe the manual regulator SSSL locus in the P-Q plane. Typically, when the power system is strong ( $X_s$  is low) the SSSL locus is outside the generator capability curve. However, on weak systems, the manual SSSL can be more restrictive than the generator capability in the underexcited region.

Under automatic operation (AVR), the voltage regulator rapidly varies the field current in response to system operating conditions. This changes the maximum value of the power angle curve upwards or downwards as required by the system. This dynamic response improves the SSSL as compared to that resulting from manual regulator operation. The effect of AVR on SSSL depends on the voltage regulator gain, the regulator time constant, and the field time constant [1] [8].

#### D. Minimum-Excitation Limiter (MEL)

Power system operation conditions or equipment failure may require generators to operate in an underexcited condition to absorb reactive power from the power system. During light system loads, transmission lines behave as reactive-power sources. Generators are required to draw excess reactive power to prevent high-voltage system conditions. An AVR failure in a generator could drive this unit to an overexcited condition and create an excess of reactive power that needs to be absorbed by nearby generators. These nearby generators may reach underexcited operating conditions.

As stated previously, three factors may limit the capability of a synchronous generator to operate in the underexcited region. In this region, core-end heating, power-system stability, or allowable operating voltage limit the generator capability to absorb reactive power.

MEL is a control function included in the automatic voltage regulator (AVR) that acts to limit reactive-power flow into the generator. During normal operation, the AVR keeps generator voltage at a preset value. When system conditions require the generator to absorb reactive power in excess of the MEL set point, the MEL interacts with the AVR to increase terminal voltage until reactive-power inflow is reduced below the setting. The MEL operating characteristic plots as a line in the P-Q plane. Fig. 3 shows the MEL characteristic as a straight line for this particular generator. For other MEL designs, the characteristic may be a curve or its approximation by linear segments, as shown in Fig. 5.

The MEL is typically set based on the most limiting of two conditions: the manual regulator SSSL or the generator underexcited capability limit [1] [4]. Fig. 6 depicts the MEL characteristic set according to this criterion. This figure corresponds to the actual generator and power system data of the Juan de Dios Batiz Paredes power station (see Appendix A). The SSSL characteristic is represented at nominal voltage. In this case, the capability curve is more restrictive than the SSSL. For weaker power systems the SSSL may be the most restrictive factor.

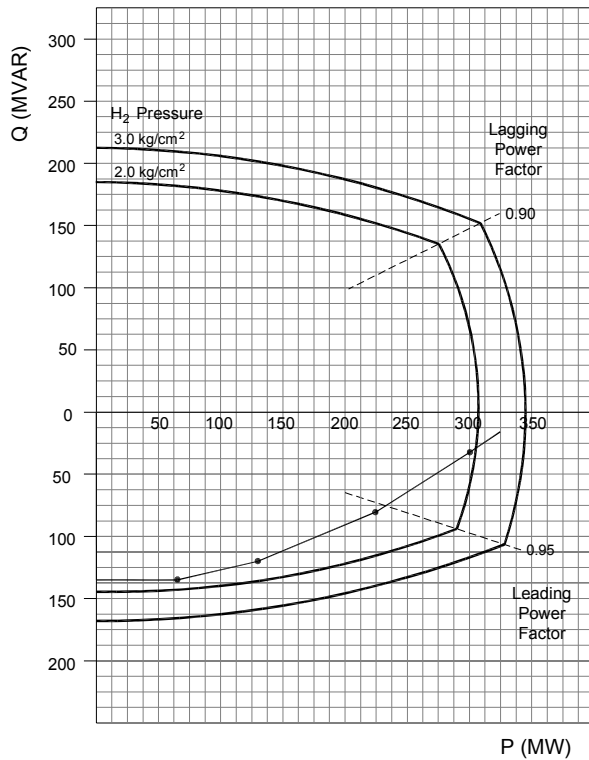


Fig. 5 Capability curve at nominal voltage of a 312 MW, 347 MVA, 20 kV, 0.9 PF, 3600 RPM, 60 Hz, hydrogen-cooled steam-turbine generator

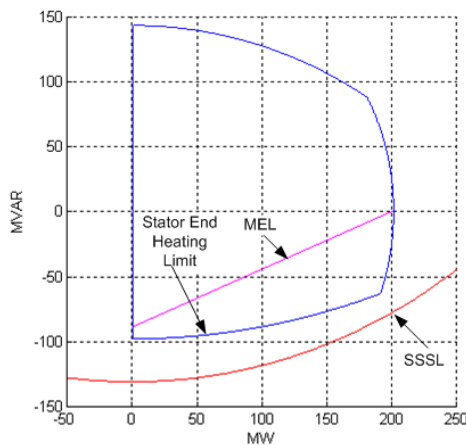


Fig. 6 Typical setting of the generator MEL

When the power system is in the recovery stage after a disturbance, there may be a need for some generators to violate the underexcited operation limit on a short-term basis. If the generator manufacturer permits this operating condition, and the MEL function could be disabled, we should detect the MEL violation and issue an alarm. The operator has the responsibility of limiting this mode of operation to prevent generator damage [1].

#### E. Overexcitation Limiter (OEL)

OEL is a control function included in the AVR that protects the generator from overheating resulting from prolonged field overcurrent. OEL detects the field-overcurrent condition

and acts with time delay to ramp down the excitation to a preset value (typically 100–110 percent of rated field current [2]). The OEL operating characteristic plots as a line in the P-Q plane. Fig. 3 shows the OEL characteristic as a straight line for this particular generator.

### III. GENERATOR PROTECTION FUNCTIONS RELATED TO THE CAPABILITY CURVE

Several generator protection functions are intended to prevent the machine from violating capability-curve limits to some extent. These protection functions are stator thermal, rotor thermal, motoring, overvoltage, undervoltage, and loss of field.

#### A. Stator-Thermal Protection

Thermal protection for the generator stator core and windings is intended to protect the generator from the overheating resulting from overload, failure of cooling systems and localized hot spots caused by core lamination insulation failures or by localized or rapidly developing winding failures [9] [10].

As mentioned before, the continuous output capability of a generator is expressed in kilovolt-amperes (kVA) available at the terminals at a specified frequency, voltage, and power factor. In general, generators may operate successfully at rated kVA, frequency, and power factor for a voltage variation of 5 percent above or below rated voltage. Under emergency conditions, the generator may exceed the continuous capability for a short time. Reference [5] expresses the armature-winding short-time thermal capability for cylindrical-rotor machines as a set of time and current pairs of values (see Table I) that define an inverse time-current curve.

TABLE I  
SHORT-TIME STATOR THERMAL CAPABILITY  
FOR CYLINDRICAL-ROTOR SYNCHRONOUS GENERATORS [5]

Time (seconds)	10	30	60	120
Armature current (percent of rated current)	218	150	127	115

Generators typically have temperature sensors (resistance temperature detectors or thermocouples) supplied by the manufacturer that measure the temperature at different points of the winding. Generator overload protection receives information from these sensors to continuously monitor winding temperature. In attended generating stations, overload protection typically issues an alarm. In unattended stations, the protection may initiate corrective action or trip the unit when preset temperature limits are exceeded.

In generators lacking temperature sensors, overload protection may be provided by a relay function responding to the measured armature current. In the past, an inverse-time overcurrent relay provided this function. The relay was coordinated with the generator short-time capability curve derived from the time-current pairs given in Table I [9]. A better solution is for the relay function to emulate the thermal behavior of the generator. This thermal-overload protection function is available in some digital generator multifunction relays.

A failure of the generator cooling system may result in rapid deterioration of the stator-core lamination insulation and/or stator-winding conductors and insulation. Generator overload protection based on temperature sensors also responds to the winding overheating that results from cooling-system failures. There may be additional sensors to monitor the coolant temperature, flow, or pressure, which may be connected to an alarm, to automatically reduce load to safe levels, or to trip. Overload protection based on the measured armature current does not provide protection against cooling system failures.

Localized hot spots in the stator core result from high eddy currents that find conducting paths across the damaged insulation between laminations. Lamination insulation may fail by generator misoperation (prolonged over- or underexcitation operation, for example), by lamination vibration, by foreign objects, or by damage to the core during installation or maintenance. Temperature sensors located at strategic positions can detect hot spots. However, detection is only partial, since it is not possible or practical to cover the entire core and windings with the detectors. At present, only large steam-turbine generators have this type of protection, which normally issues an alarm.

### B. Rotor-Thermal Protection

Thermal protection for the generator field includes protection for the main field winding circuit and protection for the main rotor body, wedges, retaining ring, and amortisseur winding [9] [10].

The field winding may operate continuously at a current no greater than that required for producing rated kVA at rated power factor and voltage. For power factors less than rated, the generator output must be reduced following the overexcited branch of the capability curve to keep the field current within these limits. Under abnormal conditions, such as short circuits and other system disturbances, the generator may exceed these limits for a short time. Reference [5] expresses the short-time thermal capability for cylindrical-rotor machines as a set of time-current pairs defining an inverse time-current curve (see Table II).

TABLE II  
SHORT-TIME ROTOR THERMAL CAPABILITY  
FOR CYLINDRICAL-ROTOR SYNCHRONOUS GENERATORS [5]

Time (seconds)	10	30	60	120
Field current (percent of rated current)	209	146	125	113

A typical rotor thermal protection element measures directly or indirectly the dc field current or voltage and operates on an inverse-time curve that coordinates with the curve resulting from the time-current pairs given in Table II.

Thermal protection of the generator rotor body is difficult to provide. Other generator protection functions prevent rotor-thermal damage, such as negative-sequence, loss-of-excitation, or loss-of-synchronism protection.

### C. Motoring Protection

Motoring of a generator takes place when the energy supply to the prime mover is cut off while the generator is on line and excited. The generator operates as a synchronous motor driving the prime mover. There is no danger for the generator in this operating condition, but the prime mover may suffer damage during motoring. In addition, the mechanical load that the prime mover presents to the generator (operating as a synchronous motor) may be high. This load represents an active-power loss for the power system.

For steam turbines, motoring causes overheating and potential damage to the turbine blades and other turbine parts. The main purpose of steam flow through a turbine is delivery of energy to rotate the rotor. This steam flow also takes out of the turbine the heat caused by winding losses resulting from the rotation of the turbine rotor and blades in a steam environment. During motoring, the blades and other turbine parts overheat, because there is no steam flow through the turbine to dissipate the heat. Steam turbines may even overheat when the generator is operating at no load or in a light load condition. Turbine manufacturers provide information on the permissible time that steam turbines may operate in a motoring condition.

Other types of prime movers may experience different problems during motoring. Hydraulic turbines may suffer cavitation of the blades on low water flow during motoring. Gas turbines may have gear problems when rotating as a mechanical load. Diesel-engine generating units are in danger of explosion and fire from unburned fuel.

Motoring protection is therefore necessary for all generating units except hydro units designed to operate as synchronous condensers [9] [10]. This external protection complements the detection means embedded in the generator control system. The most widely applied motoring protection uses a time-delayed power directional element to detect the active power reversal caused by the motoring condition. A motoring protection relay generally trips the main generator breaker(s) and the field breaker(s), transfers the auxiliaries, and provides a trip signal to the prime mover [9] [10].

The power-element setting depends on the type of prime mover. The power required to motor the unit equals the load imposed by the prime mover plus mechanical losses. Typical values in percentage of rated power are [10]: steam turbines: 0.5–3 percent; hydro turbines: 0.2–2 percent; gas turbines: up to 50 percent; diesel engines: up to 25 percent. The power-element setting range should include both negative and positive active-power values.

The power element should have a time delay to prevent misoperation for power swings caused by system disturbances or when synchronizing the machine to the system. This time delay should be below allowable turbine motoring times. Typical values are in tens of seconds.

In some hydraulic, steam, and gas turbine generating units, intentional motoring is permitted as a normal operating condition. Some examples are: motoring the unit to accelerate the rotor during starting conditions, operating a hydraulic unit as a synchronous condenser or in a pump/storage mode, and se-

quential tripping of steam-turbine units. Motoring protection should not interfere with this permissible operating condition.

#### D. Overvoltage and Undervoltage Protection

Overvoltage is an abnormal condition most likely to occur in hydrogenerators, where load rejection may cause overspeed levels of more than 200 percent of normal and significant overvoltage. Typical generator overvoltage protection includes an instantaneous voltage element set at 130–150 percent of nominal voltage and an inverse-time voltage element set at approximately 110 percent of nominal voltage. This protection typically trips the generator main breaker, trips the field breaker, and transfers unit auxiliaries [9] [10].

It is possible to detect undervoltage generator operation using an inverse-time or definite-time undervoltage element. We may set this element at approximately 95 percent of nominal voltage and use it to issue an alarm so the operator can remedy the undervoltage condition whenever possible.

#### E. Loss-of-Field Protection

A generator may totally or partially lose excitation as a result of accidental field breaker tripping, field open circuit, field short circuit (slip-ring flashover, for example), voltage regulator failure, or loss-of-excitation system supply.

##### 1) Effect of the Loss-of-Field Condition on the Generator and the Power System

When a generator loses excitation, the rotor field gradually extinguishes, and the magnetic coupling between rotor and stator magnetic fields eventually diminishes to a point where the machine loses synchronism. The rotor speed increases to a value for which the machine, operating as an induction generator, produces the active power demanded by the power system in this new condition. This value is lower than the active power delivered by the generator before losing excitation. Operating as an induction machine, the generator draws large amounts of reactive power from the system, which produces high armature-current values (in the order of two to four times rated current) and depresses the voltage. In addition, slip-frequency eddy currents induce in the rotor, having a magnitude proportional to the generated power.

When initially operating at light load, the generator may not lose synchronism as a result of the loss of field. In this case, the machine operates as a synchronous generator based on the principle of reluctance. In any case, the machine needs to receive large reactive-power amounts from the system to establish the magnetic field.

Both the machine and the power system are at risk when a generator loses excitation. The generator may suffer rotor or stator overheating, and experience large pulsating torques as a result of operating as an asynchronous machine [11]. The power system may have voltage problems.

The severity of the disturbance depends primarily on the initial generator load [1]. The impedance of an induction generator is a function of slip: the higher the slip, the lower the machine impedance. The induction-generator slip strongly depends on the generator initial load: a higher initial load produces a higher induction-generator slip value. Lower generator

impedance means higher reactive-power consumption, higher stator and rotor currents, and lower terminal voltage. The worst case is when the generator loses excitation at full load, where slip may reach values of 2–5 percent [1]. Other factors conditioning the severity of the loss-of-excitation disturbance are the system impedance and the mode-of-excitation failure.

Generator stator overheating depends on the armature-current value. As mentioned before, the worst case occurs when the generator is operating at full load when it loses excitation.

Rotor overheating depends on initial loading and the other factors just mentioned and also on the rotor design. In a cylindrical rotor, induced eddy currents circulate through the rotor body and the rotor-coil wedges. They also flow through the field circuit if the field is shorted or closed through a field discharge resistor. These currents may overheat and damage the rotor in a few seconds. Salient-pole rotors (hydro generators) typically have amortisseur windings through which induced slip frequency currents can circulate. If the amortisseur winding can withstand eddy currents, the rotor is not a limiting factor for operation as an induction generator.

There are no general guidelines on the permissible time a generator may operate without field [10]. Generator manufacturers should provide this information.

The power system is the other possible limitation to generator operation without field. The reactive-power deficit may cause a voltage collapse, especially if a large generator connected to a weak system loses excitation. Another possibility is the loss of steady-state stability, as mentioned before. When these problems arise, the system may lose voltage or synchronous stability in a few seconds. Voltage sag at the generator terminals during the loss-of-field condition is a good indicator of the power system not being able to withstand the disturbance.

##### 2) Protection Schemes

The previous analysis shows that synchronous generators must have some kind of loss-of-field protection in addition to the protection functions included in the excitation system. This protection should provide an early alarm to permit the operator to restore the field in the case of an accidentally tripped field breaker. After a time delay, the protection must trip the main generator breaker and the field breaker (to minimize damage in cases of field short circuits or slip-ring flashovers), and transfer unit auxiliaries. In some cases it may be necessary to trip the turbine stop valves also.

Generator loss-of-field protection has received special attention [9] [10] [12]–[14]. Mason [12] introduced the concept of using a “distance element of the so called mho family” to detect loss of field; the relay receives the generator terminal voltage and current as input signals. This offset mho element characteristic is depicted in Fig. 7, showing the originally recommended settings: a circle diameter equal to the synchronous reactance  $X_d$ , and a negative offset equal to half the direct-axis transient reactance ( $-X_d' / 2$ ).

The apparent impedance measured by the relay when the generator loses the field describes a trajectory in the impedance plane (see Fig. 7) that starts at the impedance value cor-

responding to the generator initial load. This point is in the first quadrant of the impedance plane when the generator initially operates in a lagging condition (delivering reactive power), or it is located in the fourth quadrant when the generator initially operates in a leading condition (consuming reactive power).

The apparent impedance does not reach a final constant value when the machine gets to the new steady state after losing excitation. The apparent-impedance value corresponds to the active power delivered and reactive power consumed by the generator operating as an induction generator in the new steady-state condition. This impedance value depends on slip and hence on the initial load value. In the steady state the induction-generator slip oscillates. As a result, active and reactive power and the apparent impedance value also vary with time. The apparent impedance describes a first loop in the fourth quadrant (corresponding to the first pole slip), as shown in the real impedance trajectory depicted in Fig. 7, and continues to oscillate in this region.

When the generator is initially operating at full load, the first apparent-impedance loop occurs around a point with a resistance value determined by the average active power delivered by the induction generator and with a reactance value that is close to the average of the generator d-axis and q-axis transient reactances ( $X_d'$  and  $X_q'$ ). On the other hand, for the generator operating initially at no load, generally there is no loss of synchronism, and the first loop apparent-reactance value will vary in between the d-axis and q-axis synchronous reactances ( $X_d$  and  $X_q$ ). For other initial-load conditions, the first pole slip produces an impedance loop in a region with reactance values between those of the full-load and no-load initial conditions. This is the case shown in Fig. 7. However, as subsequent oscillation cycles take place, the impedance locus moves in a larger area of the impedance plane, as we will see in the simulation results presented in Section V.

During stable and unstable power swings, the impedance measured by the loss-of-field relay also describes a trajectory in the impedance plane. The relay may misoperate if the trajectory penetrates the operating characteristic. A small relay characteristic may prevent excursions of the power swing impedance trajectory in the relay operating region. However, the practice is to enhance security for power swings by delaying operation of the loss-of-field relay. A time delay of approximately 0.5–0.6 s is generally adequate [10] [13], but transient stability simulation studies to determine relay time-delay settings are highly recommended.

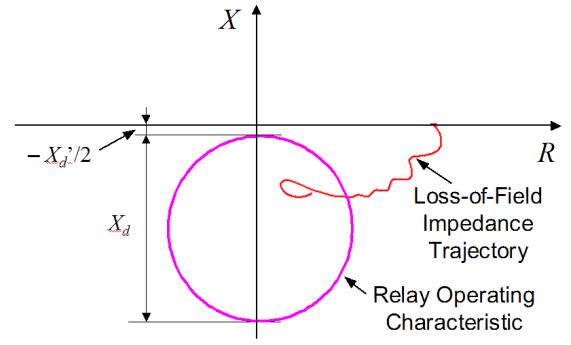


Fig. 7 Loss-of-field protection using a negative-offset mho element

For the generator reactance values that existed when Mason introduced the offset mho characteristic for loss-of-field protection ( $X_d$  was in the range of 1.1 to 1.2 p.u.), the settings shown in Fig. 7 normally provided detection of loss of excitation conditions for any initial generator loading. These settings also ensured relay security for power swings without requiring a time delay.

Modern generators have larger reactance ( $X_d$  is typically about 1.5–2 p.u.). The larger relay characteristic may infringe on the underexcited branch of the capability curve and prevent fully using the machine capability in this region. The initial recommendation, of reducing the characteristic diameter to 1 p.u., limited loss-of-field detection only to cases of high initial generator loading. Later, the distance element concept was enhanced using two negative-offset mho element characteristics [13]. Fig. 8 illustrates the enhanced characteristic suitable for generators with large direct axis reactance. Zone 1 serves to detect loss of field for high load conditions (the most severe condition for both the generator and the system). A time delay of about 0.1 s [10] provides security against transients. Zone 2 detects loss of excitation for light loads and operates with time delay to override power swings. A time delay of 0.5–0.6 s should provide security for power swings. However, it is recommended to set this element based on transient stability studies.

The settings shown in Fig. 7 and Fig. 8 for the negative-offset loss-of-field element [10] [13] do not take into account the generator capability curve, the steady-state stability characteristic, and the MEL characteristic.

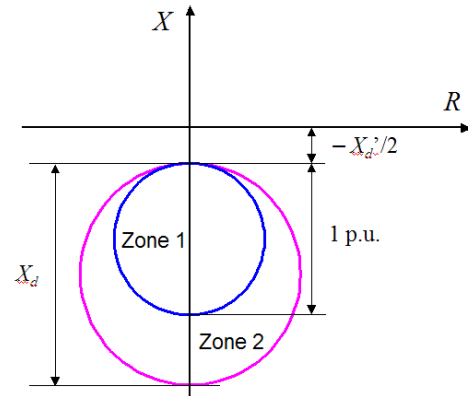


Fig. 8 Two-zone loss-of-field protection using negative-offset mho elements

Tremaine and Blackburn [14] introduced a characteristic that uses a combination of a positive-offset mho element and a directional element. With the setting shown in Fig. 9 [10], this characteristic is just outside the SSSL characteristic, to prevent the system from going unstable. However, this setting does not consider the capability curve and the MEL characteristic. System impedance  $X_s$  in Fig. 9 includes the step-up transformer impedance plus the system equivalent impedance. The directional element provides security for close-in external faults. This scheme should issue an alarm, allowing the operator to correct the low- or lost-excitation condition [10]. The scheme should also initiate time-delayed tripping. A typical time-delay setting range is 10 s to 1 minute [7].

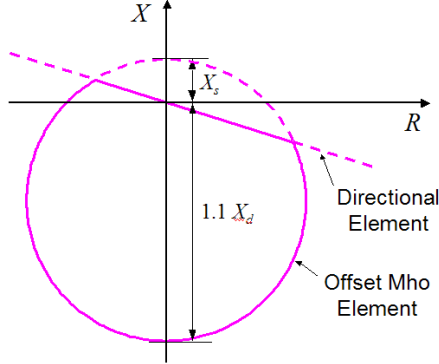


Fig. 9 Loss-of-field protection using a positive-offset mho element supervised by a directional element

This concept was enhanced using an additional negative-offset mho element [9] [10] to protect generators with large direct axis reactance values. Fig. 10 illustrates the enhanced two-zone characteristic. Zone 1 should have a time delay of 0.2 to 0.3 s to override power swings and other transients. Zone 2 should issue an alarm and initiate time-delayed tripping, with 1 minute as a typical delay.

The one-zone and two-zone positive-offset schemes (Fig. 9 and Fig. 10) also include an undervoltage element (typically set to 0.8–0.9 of generator nominal voltage) to monitor the effect of the loss of excitation on the power system. A low-voltage condition means that the system may collapse. The undervoltage element operates to accelerate Zone 2 tripping in this case. A typical time delay is 0.25–1 s. The shorter time delay is recommended for the one-zone scheme and the longer time delay for the two-zone scheme [10]. On the other hand, a normal voltage condition means that the system withstands the generator loss-of-excitation condition. There is no need for accelerating Zone 2 operation in this case.

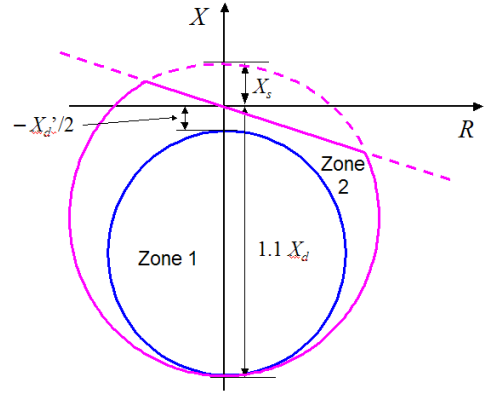


Fig. 10 Two-zone loss-of-field protection using positive- and negative-offset mho elements supervised by a directional element

We have to plot the capability curves, MEL, and SSSL characteristics in the impedance plane in order to analyze the operation of the loss-of-field protection relays that have the characteristics shown in Fig. 7 through Fig. 10. Every point of these curves in the P-Q plane plots as a point in the impedance plane at a given voltage magnitude.

A given apparent complex power  $Se^{j\phi}$  value corresponding to an angle  $\phi$  in the complex P-Q plane plots as an impedance  $Ze^{j\phi}$  with the same angle in the impedance plane; the impedance magnitude  $Z$  depends on  $S$  and the generator terminal voltage  $V_t$  [7] [15]:

$$\bar{Z} = \frac{V_t^2}{S} (\cos \phi + j \sin \phi) = \frac{V_t^2}{S} e^{j\phi} \quad (12)$$

With  $V_t$  expressed in kV and  $S$  in MVA, (12) gives the impedance value in primary ohms. We obtain the impedance value in secondary ohms by multiplying the impedance value in primary ohms by the current transformer ratio CTR and dividing the result by the voltage transformer ratio VTR.

Fig. 11 depicts the impedance plane representation of the capability curve and MEL characteristic of a 202 MW generator. Impedance values are expressed in secondary ohms at the generator voltage. The generator capability curve corresponds to that of Fig. 3 with a generator hydrogen pressure of 206 kPa; it is plotted at nominal voltage in the impedance plane. Fig. 11 also shows the SSSL characteristic at nominal voltage. Notice that in the impedance plane, the forbidden operation region is inside the curves.

The generator has a positive-offset, two-zone loss-of-field protection scheme, including an undervoltage element that accelerates Zone 2 operation for low-voltage conditions during the loss-of-field event. Fig. 11 also shows the relay characteristic with the actual settings, which coincide with those shown in Fig. 10. For simplicity, the directional element is not shown. From Fig. 11, it is clear that Zone 2 of the relay characteristic is set just outside the SSSL characteristic to prevent the system from losing steady-state stability. However, the relay characteristic is inside the capability curve in this case. This leaves a region between the relay characteristic and the capability curve where the generator is not protected [16]. If a partial loss-of-field condition results in an impedance value

that stays in this region long enough, the generator may suffer damage.

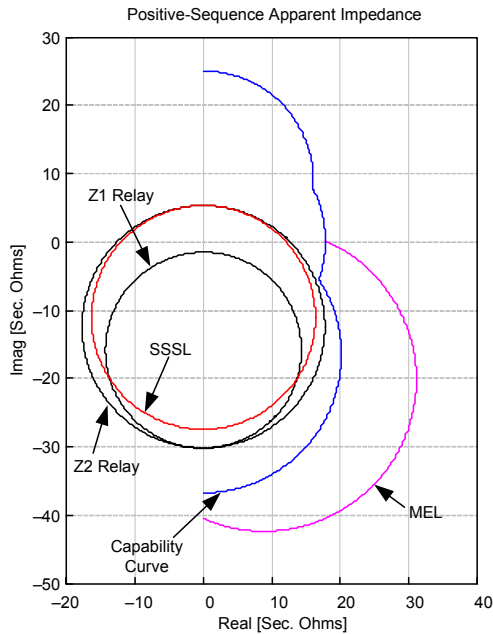


Fig. 11 Impedance-plane representation of generator capability curve, MEL, SSSL, and loss-of-field relay characteristic. The relay is set according to Fig. 10 to prevent the system from losing steady-state stability.

For better generator protection, the loss-of-field element should be set to allow MEL to operate, to prevent the system from losing steady-state stability, and to protect the generator from stator-end region damage, as shown in Fig. 12. This figure shows the capability curve and MEL characteristic of a 312 MW generator. The capability curve, represented in the impedance plane at nominal voltage, is that of Fig. 5 with a generator hydrogen pressure of 3 kg/cm<sup>2</sup>. Impedance values are expressed in primary ohms at the generator voltage.

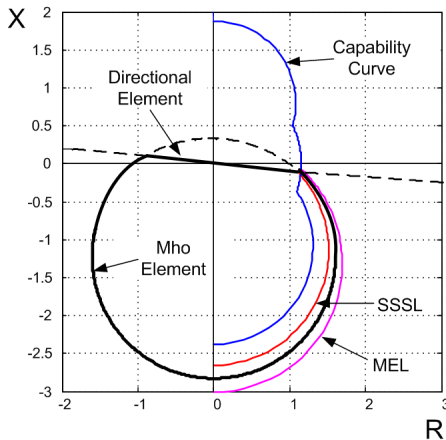


Fig. 12 Impedance-plane representation of generator capability curve, MEL, SSSL, and the loss-of-field relay characteristic. The relay is set to protect the generator from stator-end heating damage and to prevent the system from losing steady-state stability.

Fig. 13 depicts a P-Q plane representation of the characteristics shown in Fig. 11. The generator capability curve and the MEL characteristics are taken directly from Fig. 3. This is an advantage of the P-Q plane representation. The SSSL and re-

lay characteristics are plotted at nominal voltage. The SSSL characteristic plots as a circle in the P-Q plane, according to (10) and (11).

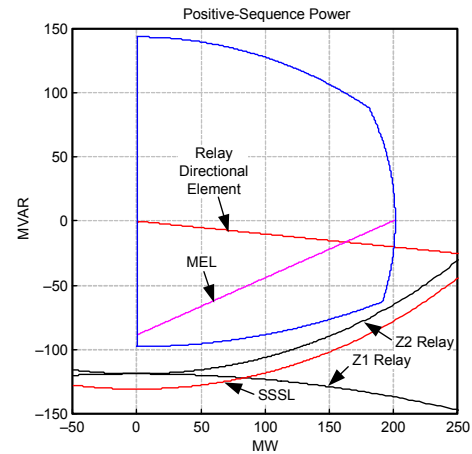


Fig. 13 P-Q plane representation of generator capability curve, MEL, SSSL, and loss-of-field relay characteristic. The relay is set according to Fig. 10 to prevent the system from losing steady-state stability.

Fig. 13 also shows the two-zone relay characteristic. We can see that Zone 2 of the relay characteristic is a circle both concentric with and inside the SSSL circle as a result of the setting shown in Fig. 10. As mentioned before, this prevents the system from losing steady-state stability but leaves the generator unprotected according to the capability curve.

Application of offset mho elements is the most common solution to loss-of-field protection today. However, using an element having a linear characteristic in the P-Q plane (see Fig. 14) has also been proposed [7] [17]. This characteristic translates into an offset circular characteristic in the impedance plane.

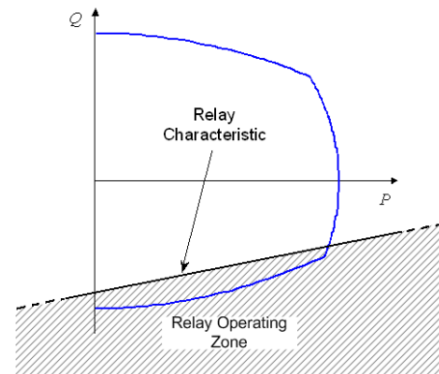


Fig. 14 Loss-of-field relay having a linear characteristic in the P-Q plane

In a practical implementation of this solution [17], it is recommended to set the characteristic following the generator capability curve, the SSSL characteristic, or the MEL characteristic as defined by the user. The loss-of-field element is supervised by an undervoltage element and an overcurrent element. If only the loss-of-field element operates, the relay issues an alarm. If, additionally, the undervoltage element and/or the overcurrent element operate, the relay initiates time-delayed tripping. The operating time follows an inverse

law as a function of the generator armature current, ending with a minimum definite-time delay.

#### IV. P-Q PLANE-BASED GENERATOR PROTECTION AND SUPERVISION

A digital design provides the flexibility to create relay characteristics in the P-Q plane that are tailored by the capability curve and SSSL as required. We may define a tripping characteristic for loss-of-field protection and an alarm characteristic to detect violations of the capability curve. An advantage of this scope is that we can directly use information on the generator capability curve and SSSL to set the relay. There is no need to transfer all the characteristics to the impedance plane.

##### A. Loss-of-Field Protection Characteristic

The P-Q plane-based loss-of-field protection scheme (see Fig. 15) includes a loss-of-field element, two active-power elements, and an undervoltage element (not shown Fig. 15).

The active-power elements act as blinders that restrict coverage along the P axis. This supervision increases the scheme security for power swings. The left-side active-power element characteristic coincides with the Q axis. The right-side active-power element characteristic adapts to the generator load condition: its setting is equal to the measured predisturbance active power, plus 20 percent of generator-rated active power. The upper limit of the right-side active-power element setting is the generator MVA rating; alternatively, the user may select an upper limit value, the turbine MW rating, for example.

The relay operating characteristic in the P-Q plane (see Fig. 15) is the shadowed region below the loss-of-field element characteristic and between the characteristics of the active-power elements.

When the generator operating point in the P-Q plane falls inside the relay operating region, the scheme issues an alarm signal and initiates delayed generator tripping.

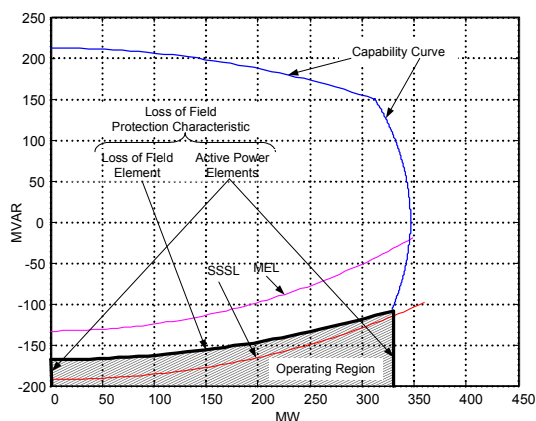


Fig. 15 Loss-of-field element characteristic in the P-Q plane set to coordinate with the generator capability curve when the SSSL characteristic is outside the capability curve

The loss-of-field element setting shown in Fig. 15 is a good choice for the case when the SSSL characteristic is outside the capability curve. In this case, we set the loss-of-field element characteristic to coincide with the capability curve to protect

the generator from stator-end core heating. This setting permits full use of the generator capability to absorb reactive power, beyond the MEL setting.

When the SSSL characteristic is inside the generator capability curve (as may occur in a weak power system), the SSSL characteristic becomes the factor that limits the amount of reactive power that the generator can absorb. In this case, we set the loss-of-field element characteristic just inside the SSSL characteristic, as shown in Fig. 16.

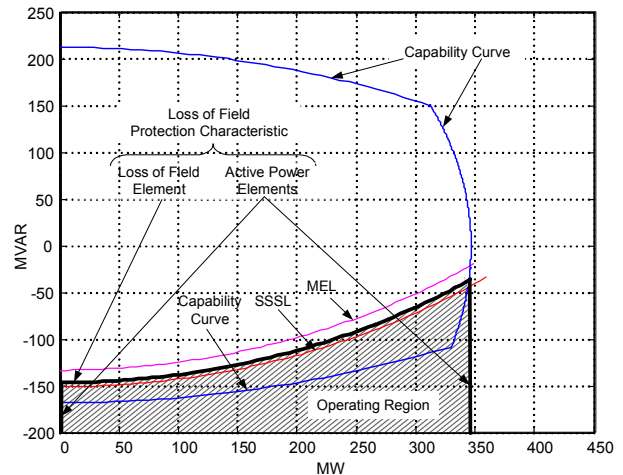


Fig. 16 Loss-of-field element characteristic in the P-Q plane set to coordinate with the SSSL when the SSSL characteristic is inside the capability curve

The P-Q plane-based protection scheme also includes an undervoltage element, typically set to 0.8–0.9 of generator nominal voltage. The undervoltage element operates to accelerate scheme operation when a low-voltage condition indicates that the system may collapse. For normal voltage conditions during the loss-of-field event, there is no need for accelerating operation, because the system is strong.

##### B. Alarm Characteristic

The alarm characteristic in the P-Q plane (see Fig. 17) is formed by the upper and right-side branches of the capability curve, by the loss-of-field element characteristic, and by an active-power characteristic that coincides with the Q axis. The alarming region is outside the characteristic. When the SSSL characteristic is outside the capability curve (as in Fig. 15), the alarm characteristic fully coincides with the generator capability curve. This is the case depicted in Fig. 17. When the SSSL characteristic is inside the capability curve (as in Fig. 16), the lower side of the alarm characteristic lies inside the capability curve, coinciding with the loss-of-field element characteristic.

Depending on the limit violated by the generator operating point (P,Q), the alarm element issues one of the following alarms:

- Armature-Current Limit Violation
- Rotor-Current Limit Violation
- Loss-of-field/Underexcitation Condition
- Motoring Condition

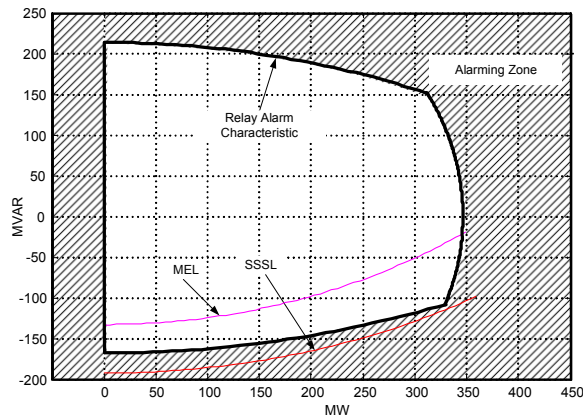


Fig. 17 The alarm characteristic is formed by the capability curve, the loss-of-field protection characteristic, and an active-power characteristic coinciding with the Q axis.

### C. Combined Characteristic

Once the generator capability curve and the SSSL characteristic have been defined, the relay characteristic can be defined. We also need to obtain measurements of the generator active- and reactive-power output values. Since this relay responds to balanced generator operating conditions, positive-sequence P and Q values are a good choice for relay quantities.

Fig. 18 depicts the relay combined characteristic for loss-of-field protection and capability-curve violation alarming. In this case, the loss-of-field element is set according to the capability curve. Measured positive-sequence P and Q values define the machine operating point in the P-Q plane. The operating point is tested against the relay characteristic to determine whether the generator is operating in normal or abnormal conditions. For an abnormal operating condition, the relay generates an alarm and, in the case of a loss-of-field condition, initiates delayed tripping.

For example, when the generator operates in a normal condition at the point  $P_A, Q_A$ , there is no relay operation or alarming. When the generator operates at the point  $P_B, Q_B$ , the relay issues an alarm indicating violation of the armature-current limit. Finally, when the generator operating condition is at the point  $P_C, Q_C$ , the loss-of-field element alarms and initiates delayed tripping.

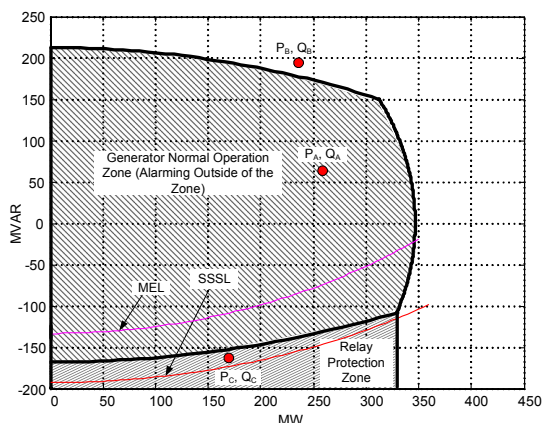


Fig. 18 Relay combined characteristic provides loss-of-field protection and capability-curve violation alarming.

### D. Setting Relay Characteristic

Fig. 19 shows the information required to define the relay characteristic, including both loss-of-field protection and capability-curve violation alarming.

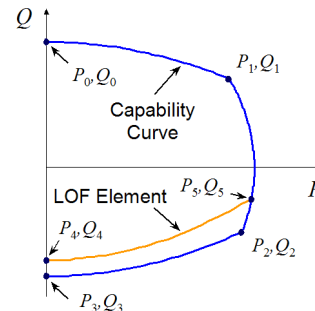


Fig. 19 P and Q points required for defining the relay characteristic

Points  $(P_0, Q_0)$ ,  $(P_1, Q_1)$ ,  $(P_2, Q_2)$ , and  $(P_3, Q_3)$  define the capability curve and also serve to define the alarm characteristic totally or partially. We may also derive point  $(P_1, Q_1)$  from the generator rated MVA and power factor data.

Points  $(P_4, Q_4)$  and  $(P_5, Q_5)$  define the loss-of-field element characteristic. For linear or circular characteristics, these two points allow making an exact representation. For other types of characteristics, we can make a fair approximation for the sake of relay setting using these two points. If required, it is possible to get a more accurate representation of the loss-of-field element characteristic by providing more pairs of P,Q points. This could be the case of a user-defined loss-of-field element characteristic.

A digital relay may automatically select the settings of the loss-of field and alarm characteristics by using the information given in Fig. 19, and also generator-impedance data and system-impedance data. To set the loss-of-field element as in Fig. 15, the relay makes point  $(P_4, Q_4)$  coincide with  $(P_3, Q_3)$  and point  $(P_5, Q_5)$  coincide with  $(P_2, Q_2)$ . To set the loss-of-field element as in Fig. 16, the relay selects the characteristic to be a circle, with points  $(P_4, Q_4)$  and  $(P_5, Q_5)$  placed just inside the SSSL circle (not shown in Fig. 19). Equations (10) and (11) define the SSSL circle.

We can select the operating relay characteristic for alarming and/or generator tripping from several (two or more) relay characteristic options based on the generator cooling-system status and generator operating conditions. Fig. 3 and Fig. 5 show capability curves for different cooling-system pressures; these curves can be used to define the relay characteristic for the different cooling conditions.

Appendix B describes methods to program into a digital relay the generator capability curve, MEL, and SSSL characteristics, using information provided by the user.

## V. GENERATOR DYNAMIC SIMULATION STUDY

### A. EMPT Model Description

The EMTP model simulates two 160 MW steam-powered units connected to the Mexican Power System (see Fig. 20) The generating units operate in the Juan de Dios Batiz Paredes thermal power station that belongs to Comisi3n Federal de

Electricidad, the national Mexican utility. This power station is interconnected with two substations of the national Mexican power system through two 230-kV transmission lines.

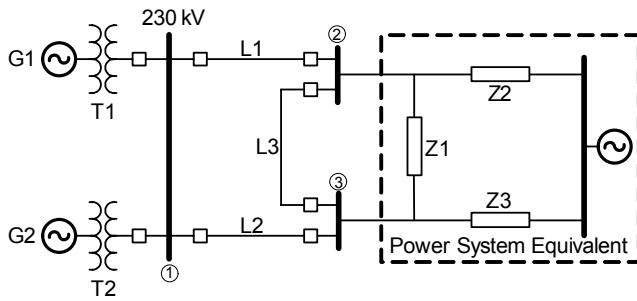


Fig. 20 One-line diagram of the power-system section of interest for digital simulation

The simulation model includes the generators and their control systems, the step-up transformers, the transmission lines, and an equivalent of the power system beyond the area of interest. Generator models include the turbine speed governor, automatic voltage regulator, and power system stabilizer (PSS) with actual transfer functions and setting values. Generator models were validated using the results of factory and commissioning tests of both units. Some protective relay functions under evaluation are also included in the simulation. Appendix A provides data on the generating units and associated power system.

For these simulations, we assume that MEL and OEL are disabled. MEL really has no effect for the loss-of-field modes considered in this study (field short circuit and field breaker opening); OEL would operate in only one case (for the other generator on line), but its operation would occur outside of the simulation time that we report.

The block diagram of Fig. 21 shows how the power-frequency and the excitation-system control loops of the generating units have been modeled in EMTP. This figure shows the relationship between the different control systems and their interaction with the turbine and the generator. The speed-droop characteristic (percentage change in frequency that would cause the output power of the units to change by 100 percent) has been set to 5 percent. Fig. 43 (Appendix A) provides additional information on the excitation-system control.

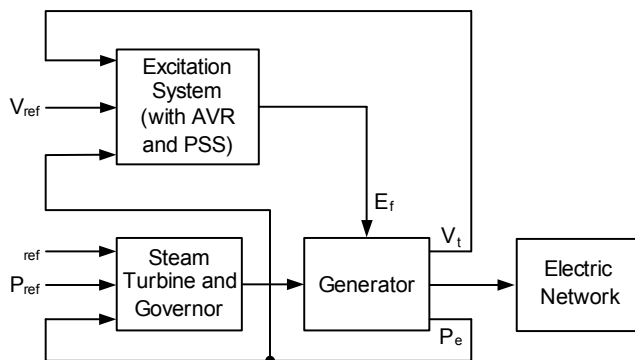


Fig. 21 Block diagram of the generating-unit power-frequency and excitation-system control loops

## B. Simulation Cases

The study includes EMTP simulation of loss-of-field and loss-of-synchronism conditions of one of the two 160 MW units for five different cases. The study covered the following groups of cases:

1. Two different initial load conditions in the generator that loses excitation: 40 MW (25 percent of rated active power) and 150 MW (94 percent of rated active power).
2. Two different modes of loss of field:
  - a. Field short circuit (slip-ring flashover, for example).
  - b. Field breaker opening during normal operation (human error or interlock override, for example). Breaker opening leaves a  $0.2 \Omega$  discharge resistor connected in the field circuit. This resistance value is very close to that of the field circuit.
3. Two different initial operating conditions in the power station: one generator and two generators on line.

The next section presents and discusses the simulation results for five of the cases analyzed in this study:

- Case 1: Loss of excitation of one generator (with the other generator on line) because of a field short circuit while the generator is carrying 150 MW.
- Case 2: Loss of excitation of one generator (with the other generator on line) because of a field short circuit while the generator is carrying 40 MW.
- Case 3: Loss of excitation of one generator (with the other generator on line) because of a field breaker opening with discharge resistor insertion while the generator is carrying 150 MW.
- Case 4: Loss of excitation of one generator (only this generator on line) because of a field short circuit while the generator is carrying 150 MW.
- Case 5: Loss of synchronism of one generator (only this generator on line) because of a temporary external fault, without generator-control systems.

## C. Simulation Results

1) *Case 1: Loss of excitation of one generator (with the other generator on line) because of a field short circuit while the generator is carrying 150 MW.*

In this case, the loss of excitation is the result of a field short circuit when the generator is carrying 150 MW, 0 MVAR, which represents 94 percent of rated active power. Fig. 22 shows the effect of the loss of excitation on the generator positive-sequence active- and reactive-power output, terminal voltage, and armature current. The loss of field occurs at 2.1 s of simulation time.

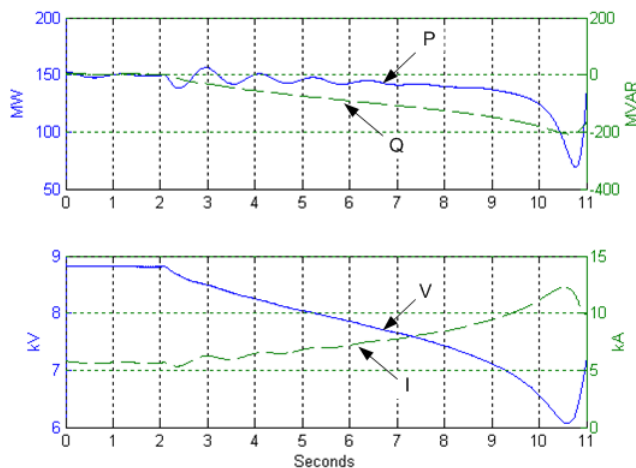


Fig. 22 Behavior of active and reactive power, armature current, and terminal voltage when the generator loses excitation because of a field short circuit while the generator is carrying 150 MW (Case 1)

Fig. 22 shows that the generator loses synchronism (significant active-power oscillations start) approximately 8 s after the loss of field. Significant oscillations take place as a result of pole slipping and the effect of saliency (different d-axis and q-axis reactance values) [1]. All these factors combine to produce slip variations during the slip cycle. In the first 7 s of machine operation without excitation (see Fig. 22), the active power diminishes slowly from 150 MW to about 135 MW until the machine loses synchronism, and then falls abruptly to approximately 70 MW in the first pole slip. Subsequent oscillations (not shown) take place around an average value of approximately 100 MW. The reactive power drawn by the generator varies almost linearly from zero to an average of -200 MVAR. As a result, the armature current grows approximately 106 percent, from 5.8 kA (0.75 p.u.) to 12 kA (1.55 p.u.). The terminal voltage drops approximately 25 percent, from 8.8 kV (1.016 p.u.) to an average value of about 6.6 kV (0.76 p.u.).

Fig. 23 depicts the impedance plane representation of Case 1, with all the values expressed in secondary ohms. This is a version of Fig. 11, but with the impedance trajectory added and the MEL characteristic eliminated for simplicity.

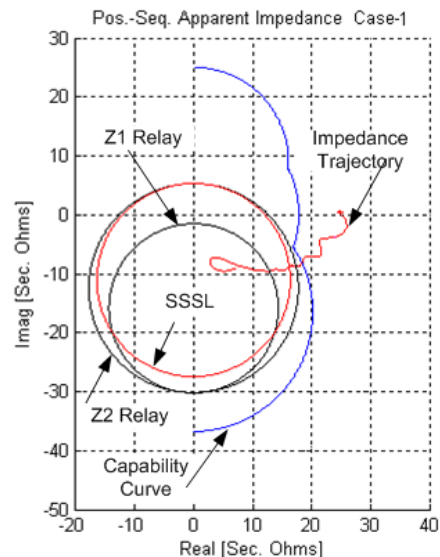


Fig. 23 Representation of Case 1 in the impedance plane. Relay characteristics are inside the capability curve. Both loss-of-field element zones operate in this case.

As mentioned with reference to Fig. 11, this generator has a positive-offset, two-zone loss-of-field protection scheme, including an undervoltage element. Fig. 23 shows the relay characteristic with the actual settings, corresponding to those shown in Fig. 10. For simplicity, the directional element is not shown. The undervoltage element is set to 87 percent of the nominal voltage, equivalent to a phase-to-ground voltage of 7.5 kV.

The impedance trajectory starts at  $(24, 0) \Omega$ . This point in the impedance plane corresponds to the initial operating condition (150 MW, 0 MVAR) in the P-Q plane. Within the simulation time frame, the impedance trajectory penetrates both zones of the relay characteristic and describes a loop around the point  $(4, -8) \Omega$ . The machine is operating as an induction generator in this region. With a setting of 7.5 kV, the undervoltage element also operates in this case. Its operation takes place 5.5 s after the loss-of-field condition (see Fig. 22).

To keep this figure simple, we only show the first 11 s of simulation time. Oscillations resulting from the out-of-step machine operation generate an oscillatory impedance trajectory after this initial stage. In Case 3, we will present 30 s of simulation and discuss this effect.

We use a three-dimension resistance-reactance-time (R-X-t) space to introduce the time variable in the impedance-plane analysis [16]. Fig. 24 shows the R-X-t representation of Case 1. The relay characteristic is a collection of circles that forms a cylinder. We only show the Zone 2 characteristic. Relay operation results from the impedance trajectory penetrating this cylinder.

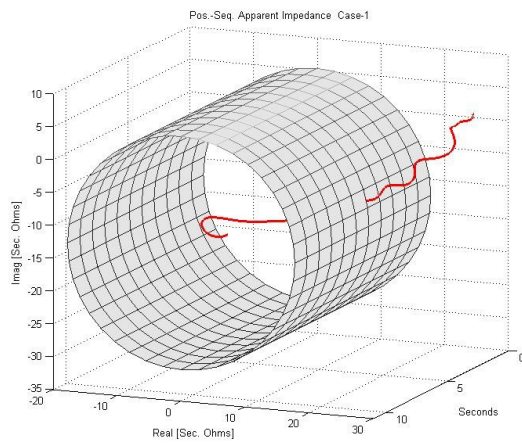


Fig. 24 Representation of Case 1 in the resistance-reactance-time space gives a three-dimension view of the loss-of-field process.

We can define the instant in which the impedance trajectory penetrates the relay characteristic by developing projections of the R-X-t space on the R-t or the X-t planes. Fig. 25 shows the projection of Fig. 24 on the R-t plane. The gray rectangle represents the loss-of-field element characteristic (Zone 2) as seen in this projection. We can see that Zone 2 initiates operation 2.9 s after the loss of field.

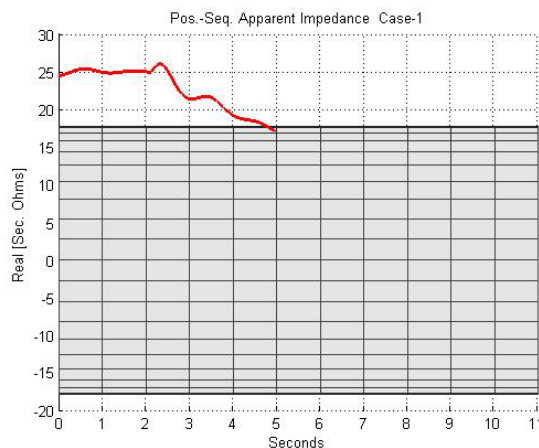


Fig. 25 Representation of Case 1 in the resistance-time plane (projection of Fig. 24 on the R-t plane) shows the instant in which the impedance trajectory penetrates the Zone 2 characteristic.

Fig. 26 depicts a P-Q plane representation of Case 1. This figure is a version of Fig. 13, but without the traditional loss-of-field relay characteristics and including the P-Q plane-based loss-of field element characteristic. Fig. 26 also shows the loss-of-excitation P-Q trajectory. The small variation of active power and the significant variation of reactive power in this time span translate into an almost vertical loss-of-field trajectory in the P-Q plane.

The right-side active-power element of the P-Q plane-based loss-of-field element adaptively sets to 182 MW, resulting from the initial load of 150 MW plus 20 percent of the rated power of 160 MW (see Fig. 26). The loss-of-field element, set to coincide with the capability curve in this case (the SSSL characteristic is outside the capability curve), detects the loss-of-excitation condition, issues an alarm, and initiates de-

layed tripping. The active-power elements restrict the operating zone just to the area needed to reliably detect the loss-of-field condition. Hence, the loss-of-field element operating zone fits very well to the almost vertical loss-of-field P-Q trajectory.

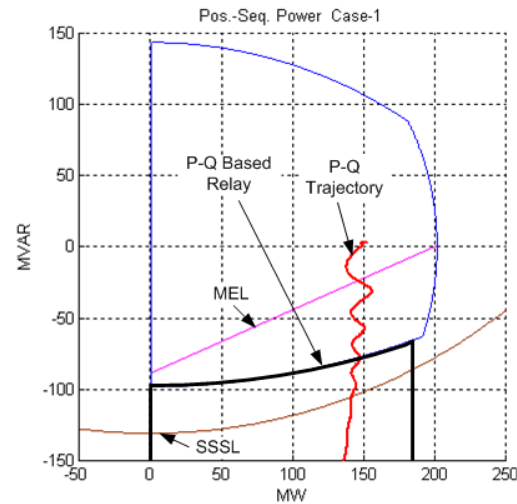


Fig. 26 Representation of Case 1 in the P-Q plane. The P-Q plane-based loss-of-field element characteristic is set to coincide with the generator capability curve. The loss-of-field P-Q locus describes an almost vertical trajectory.

2) *Case 2: Loss of excitation of one generator (with the other generator on line) because of a field short circuit while the generator is carrying 40 MW.*

This case serves to analyze the effect of the initial load when compared to Case 1. The generator loses excitation at a load of 40 MW, 0 MVAR, which is 25 percent of rated active power. Fig. 27 shows that, after some small initial oscillations, the generator gets to a new steady state without losing synchronism, and remains operating as a synchronous generator based on the reluctance principle. The reluctance torque resulting from machine saliency ( $X_d \neq X_q$ ) allows this cylindrical-rotor generator to deliver 25 percent of rated load without losing synchronism. However, because the generator lost excitation, it needs to draw reactive power from the system to establish an armature-reaction magnetic flux.

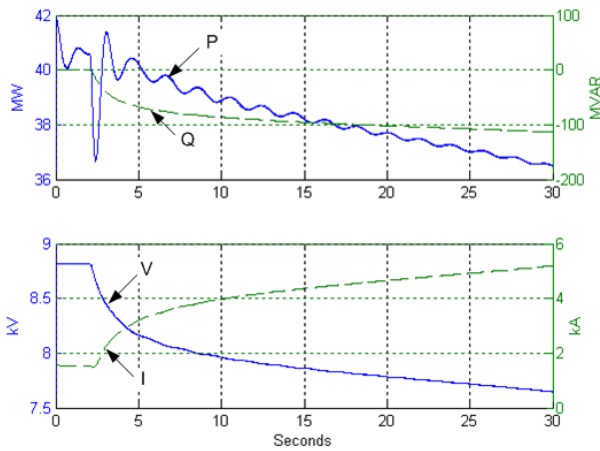


Fig. 27 Behavior of active and reactive power, armature current, and terminal voltage when the generator loses excitation because of a field short circuit while the generator is carrying 40 MW (Case 2)

In this case (see Fig. 27), the active power falls from 40 MW to approximately 36.5 MW in 30 s, and the reactive power drawn by the generator varies from zero to -110 MVAR. As a result, the armature current grows from 1.52 kA (0.195 p.u.) to 5.2 kA (0.67 p.u.) and remains below nominal current. The terminal voltage drops approximately 13 percent, from 8.82 kV (1.018 p.u.) to 7.652 kV (0.88 p.u.). It is clear from these results that a loss of field with light load is much less stressful for both the generator and the power system than a loss of field with high load.

Fig. 28 depicts the impedance plane representation of Case 2. The impedance trajectory starts at the point (90, 0) Ω (not shown in the figure), corresponding to the initial operating condition (40 MW, 0 MVAR) in the P-Q plane. The impedance trajectory penetrates both zones of the relay characteristic and ends at the point (7, -23) Ω. The machine operates as a reluctance synchronous generator in this region. The undervoltage element, set to 7.5 kV, does not operate in this case (see Fig. 27).

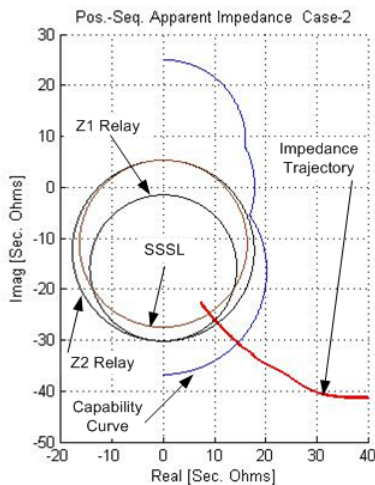


Fig. 28 Representation of Case 2 in the impedance plane; both loss-of-field element zones operate

Fig. 29 shows the R-X-t representation of Case 2. We further projected the simulation in Fig. 29 on the R-t plane (not

shown) and determined that Zone 2 initiated operation 14 s after the loss-of-field.

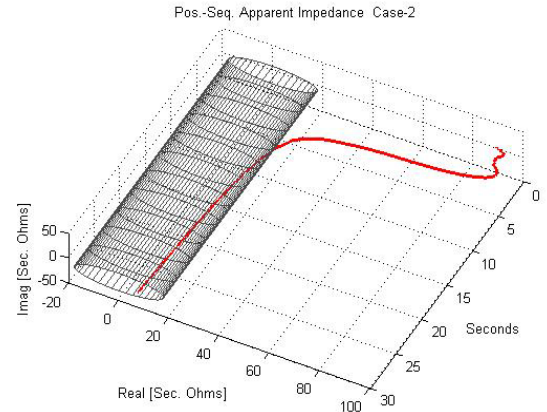


Fig. 29 Representation of Case 2 in the resistance-reactance-time space showing the impedance trajectory for 30 s

Fig. 30 depicts a P-Q plane representation of Case 2, including the P-Q plane-based loss-of-field element characteristic. As in the previous case, the loss-of-excitation trajectory is almost vertical in the P-Q plane. The right-side active-power element of the P-Q plane-based loss-of-field element assumes in this case a setting of 72 MW, resulting from the initial load of 40 MW plus 20 percent of the rated power. Again, the relay operating zone fits very well to the loss-of-field P-Q trajectory. The loss-of-field element detects the P-Q trajectory leaving the generator capability curve, issues an alarm, and initiates delayed tripping.

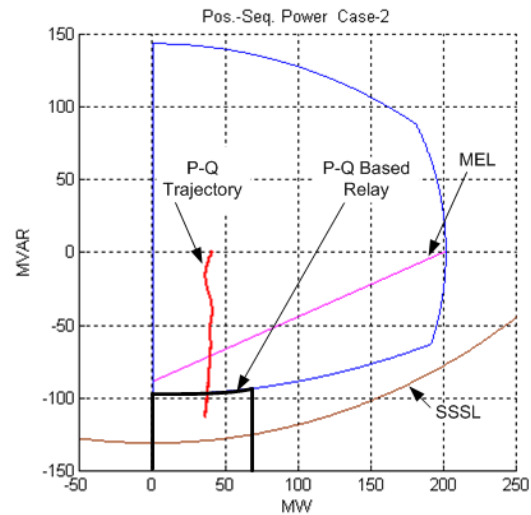


Fig. 30 Representation of Case 2 in the P-Q plane. The right-side active-power element adaptively sets to the generator initial load. The P-Q trajectory is almost vertical.

3) Case 3: Loss of excitation of one generator (with the other generator on line) because of a field breaker opening with discharge resistor insertion while the generator is carrying 150 MW.

This case serves to analyze the effect of the breaker discharge resistor inserted in the field as compared to a field short circuit (Case 1). The generator loses excitation at a load of 150 MW, 0 MVAR (94 percent of rated active power) be-

cause of a field breaker opening with insertion of a 0.2 discharge resistor in the field circuit. Fig. 31 shows that the generator loses synchronism around 4 s after the loss of field. The reactive power falls abruptly to negative values even before the loss of synchronism, indicating that the magnetic field disappears rapidly, and then starts oscillating. The effect of the discharge resistor is to reduce the time constant of the exponentially decaying magnetic flux, thus accelerating the loss of synchronism.

Fig. 31 shows 30 s of simulation time. It is therefore possible to observe several cycles of the machine oscillatory transient process while operating as an induction generator. The oscillation amplitude and frequency decrease with time as a result of the machine governor taking action to control speed. In this case (see Fig. 31), the active power falls from 150 MW to approximately 50 MW in 30 s, and the reactive power drawn by the generator varies from zero to approximately -125 MVAR. The armature current, after relatively large oscillations, reaches an average value of 6 kA (0.77 p.u.), very close to the initial value of 6.8 kA (0.75 p.u.). However, in 30 s the terminal voltage drops approximately 14 percent, from 8.8 kV (1.016 p.u.) to an average value of about 7.5 kV (0.87 p.u.).

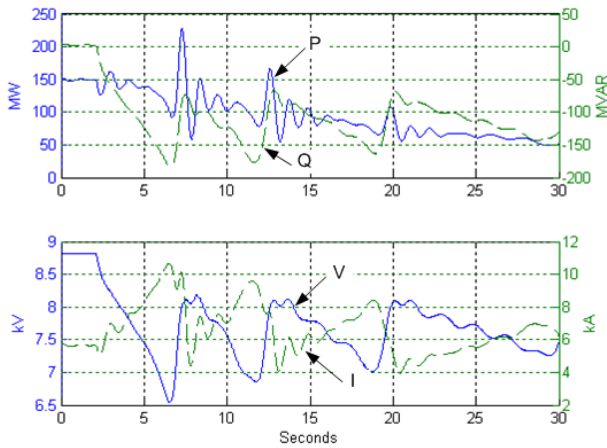


Fig. 31 Behavior of active and reactive power, armature current, and terminal voltage when the generator loses excitation by field breaker opening with discharge resistor insertion while the generator is carrying 150 MW (Case 3)

Fig. 32 depicts the impedance-plane representation of Case 3. As in Case 1, the impedance trajectory starts at (24, 0)  $\Omega$ , corresponding to the initial operating condition (150 MW, 0 MVAR) in the P-Q plane. During the 30 s of simulation time that we show, the impedance trajectory reflects the result of several cycles of machine oscillations after losing synchronism. After penetrating both zones of the relay characteristic for the first time and making a loop around the point (6, -9)  $\Omega$ , the impedance trajectory oscillates, and moves into and out of the relay characteristic several times. In real life, loss-of-field protection operates before 30 s and trips the machine. Hence, the impedance trajectory ends before 30 s. The undervoltage element, set to 7.5 kV, operates 2.9 s after the loss of field (see Fig. 31).

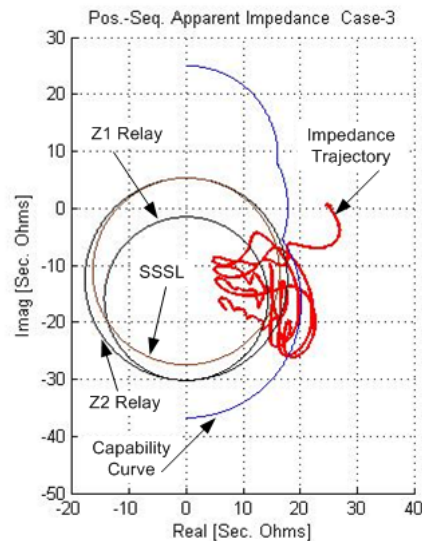


Fig. 32 Representation of Case 3 in the impedance plane. The impedance trajectory moves into and out of the relay characteristic as the generator oscillates.

Fig. 33 shows the R-X-t representation of Case 3. We further projected the simulation in Fig. 33 on the R-t plane (not shown) and determined that Zone 2 initiated operation 1.36 s after the loss-of-field. In this case, Zone 2 starts operating before the generator loses synchronism as a result of the rapid magnetic-flux decaying process, which then resulted in a rapid increase of the reactive power drawn by the generator.

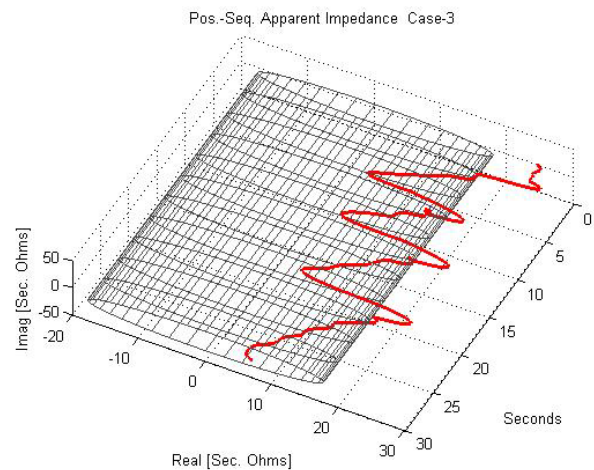


Fig. 33 Representation of Case 3 in the resistance-reactance-time space showing impedance oscillations

Fig. 34 depicts a P-Q plane representation of Case 3. The loss-of-excitation P-Q trajectory descends rapidly and almost vertically to penetrate the P-Q plane-based loss-of-field element characteristics before starting to oscillate.

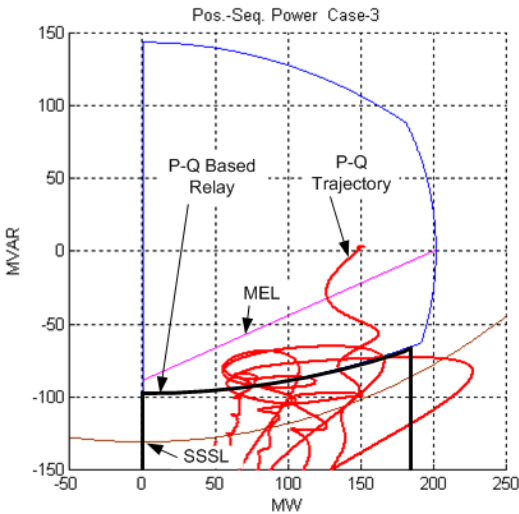


Fig. 34 Representation of Case 3 in the P-Q plane; P-Q trajectory reflects machine oscillations

4) Case 4: Loss of excitation of one generator (only this generator on line) because of a field short circuit while the generator is carrying 150 MW.

This case serves to analyze the effect of having only one generator on line at the moment of the loss of field, as compared to Case 1, in which there are two generators on line. The generator loses excitation at a load of 150 MW, 0 MVAR (94 percent of rated active power). Fig. 35 shows that the generator loses synchronism approximately 7 s after the loss of field, 1 s faster than with two generators on line.

In this case (see Fig. 35), the active power falls from 150 MW to approximately 60 MW in the first pole slip, and then oscillates around an average value of 100 MW (not shown in the figure). The reactive power drawn by the generator varies from zero to an average of -150 MVAR. Recall that in Case 1 the other generator injects reactive power to support voltage and the generator that lost the field needs to draw up to -200 MVAR. The armature current grows approximately 80 percent from 5.8 kA (0.75 p.u.) to an average value of about 10.5 kA (1.35 p.u.). The terminal voltage drops approximately 35 percent, from 8.8 kV (1.016 p.u.) to an average value of about 5.7 kV (0.66 p.u.). This voltage drop, higher than that in Case 1, results from not having a neighboring generator to support voltage.

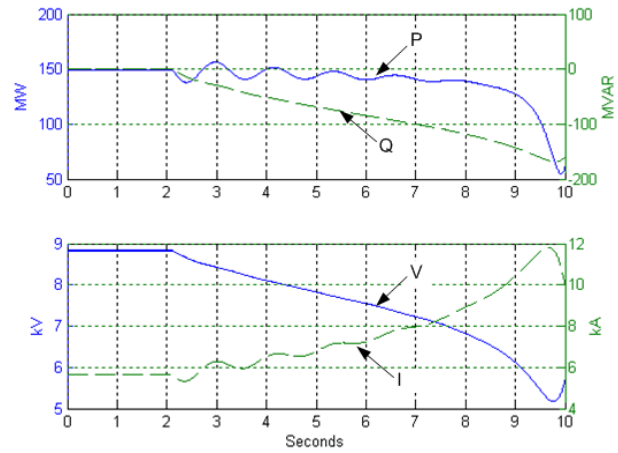


Fig. 35 Behavior of active and reactive power, armature current, and terminal voltage when the generator loses excitation because of a field short circuit while the generator is carrying 150 MW with only one generator on line (Case 4)

Fig. 36 depicts the impedance plane representation of Case 4. As in Cases 1 and 3, the impedance trajectory starts at  $(24, 0) \Omega$ , corresponding to the initial operating condition (150 MW, 0 MVAR) in the P-Q plane. Within the simulation time frame, the impedance trajectory penetrates both zones of the relay characteristic and initiates a loop around the point  $(3, -7) \Omega$  when the machine loses synchronism.

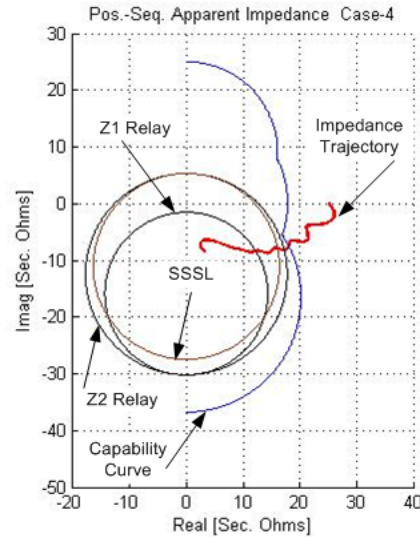


Fig. 36 Representation of Case 4 in the impedance plane; both loss-of-field element zones operate

Fig. 37 shows the R-X-t representation of Case 4. We further projected the simulation in Fig. 37 on the R-t plane (not shown) and determined that Zone 2 initiated operation 2.9 s after the loss-of-field.

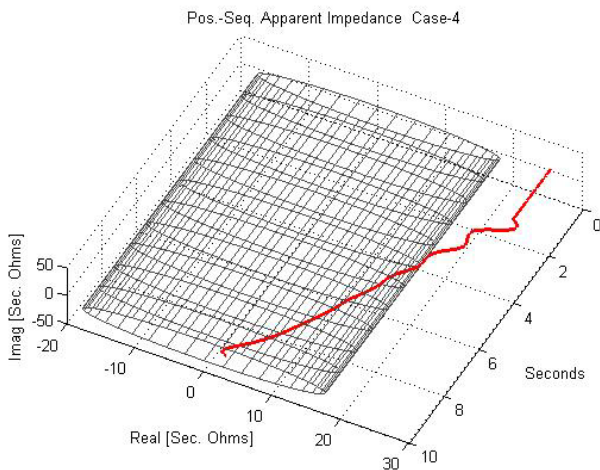


Fig. 37 Representation of Case 4 in the resistance-reactance-time space

Fig. 38 depicts a P-Q plane representation of Case 4. The loss-of-excitation P-Q trajectory descends almost vertically and penetrates the P-Q plane-based loss-of-field element characteristic.

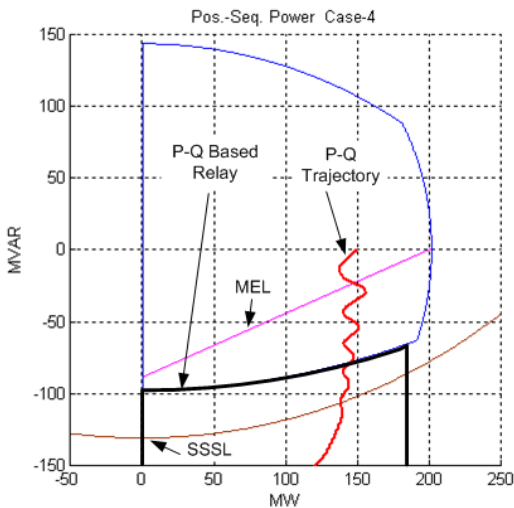


Fig. 38 Representation of Case 4 in the P-Q plane

5) *Case 5: Loss of synchronism of one generator (only this generator on line) because of a temporary external fault, without generator control systems.*

In this case, the generator loses synchronism as a result of an external temporary three-phase fault. In the prefault condition there is only one generator on line, carrying 155 MW, 0 MVAR. Generator AVR, speed control, and power-system stabilizer are out of operation in this simulation. We represent the power system in this simulation as an ideal voltage source in series with a reactance  $X_s$  of 0.374 primary ohms at 15 kV.  $X_s$  includes the generator step-up transformer and the power-system equivalent. The critical clearing time for this system configuration is 190 ms. In this case, we applied the fault during 191 ms for the system to become unstable. Fig. 39 shows the effect of the loss of synchronism on the generator positive-sequence active and reactive-power output, terminal voltage, and armature current.

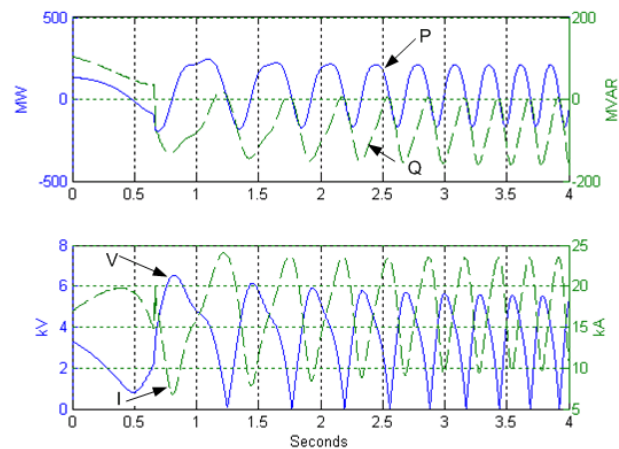


Fig. 39 Behavior of active and reactive power, armature current, and terminal voltage when the generator loses synchronism as a result of a temporary external fault (Case 5)

Fig. 39 shows the oscillations of all variables resulting from the out-of-step condition. The active power varies between 200 and  $-150$  MW, and the reactive power oscillates between 0 and  $-150$  MVAR. As a result, the armature current varies between 8 and 23 kA (1.03 to 2.96 p.u.) and the terminal voltage oscillates between 0 and 6.2 kV (0 to 0.72 p.u.). The fact that the terminal voltage drops to zero once per oscillation cycle indicates that the relay is located at the system electrical center. Fig. 39 also shows that the slip frequency grows with time as a result of the rotor acceleration increasing with every new pole slip.

Fig. 40 depicts the impedance-plane representation of Case 5. The impedance locus describes the typical circular loops of an unstable two-machine power system. There are multiple penetrations of the impedance trajectory in the relay Zone 1, one per oscillation cycle. The impedance locus is always inside Zone 2, but the directional element (not shown in Fig. 40) resets this zone almost once per oscillation cycle. Given the prevailing low-voltage condition, the undervoltage element, set to 7.5 kV, operates at the beginning of the out-of-step condition (see Fig. 39). Time delay of both zones should prevent relay misoperation for this unstable power swing.

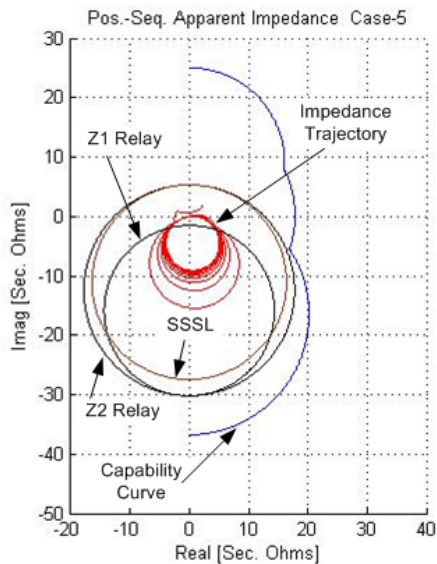


Fig. 40 Representation of Case 5 in the impedance plane. The impedance locus describes the typical circular loops of an unstable two-machine power system.

Fig. 41 shows the R-X-t representation of Case 5. Again, it is clear that the trajectory stays inside Zone 2, which is the only zone represented in this figure.

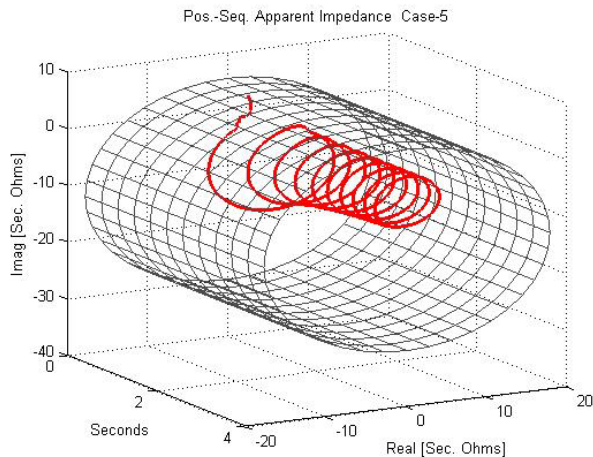


Fig. 41 Representation of Case 5 in the resistance-reactance-time space showing the result of system unstable oscillations

Fig. 42 depicts a P-Q plane representation of Case 5, including the traditional and the P-Q plane-based loss-of-field element characteristics. Traditional relay characteristics are represented at nominal voltage. Oscillations of active and reactive power describe almost elliptical trajectories in this plane. Fig. 42 clearly shows the advantage of the active-power elements acting as blinders to restrict relay coverage along the active-power axis. The loss-of-field P-Q trajectories spend less time inside the P-Q plane-based loss-of-field element operating zone than they would spend inside the traditional relay operating zone. Hence, the active-power blinders provide an inherent security for power swings to the P-Q plane-based loss-of-field element.

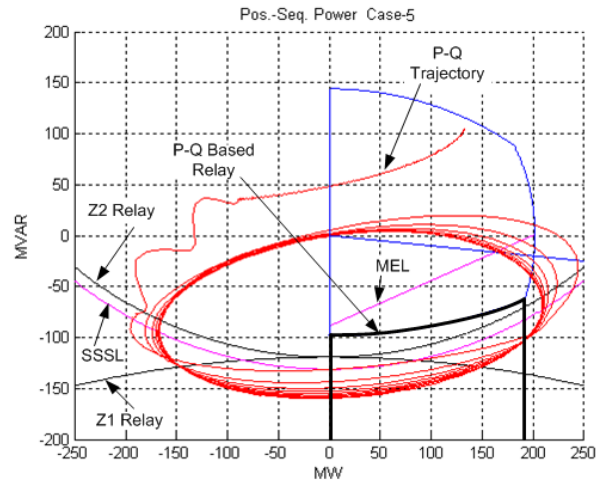


Fig. 42 Representation of Case 5 in the P-Q plane. The P-Q locus describes almost elliptical trajectories. Active-power blinders provide security for power swings to the loss-of-field P-Q plane-based element.

## VI. CONCLUSIONS

1. The following factors limit the active and reactive power that a generating unit can deliver to the power system under given operating conditions:
  - a. The generator capability curve (determined by the machine design)
  - b. Voltage limits
  - c. Power system stability limits
  - d. Minimum excitation limiter (MEL)
  - e. Overexcitation limiter (OEL)
2. Traditional rules for determining generator loss-of-field settings may result in settings that do not provide proper generator protection for certain operating conditions.
3. Providing proper settings for the loss-of-field relay requires knowledge of the generator capability curve and SSSL characteristic.
4. A digital relay design provides the flexibility for creating relay characteristics in the P-Q plane for loss-of-field protection and for capability-curve violation alarming. These characteristics are tailored by the capability curve and the SSSL, as required.
5. The P-Q plane-based loss-of-field protection scheme includes the following elements:
  - a. One loss-of-field element with a characteristic that fits to the most limiting of two curves: the capability curve or the SSSL characteristic.
  - b. Two active-power elements that act as blinders to enhance scheme security for power swings.
  - c. One undervoltage element that accelerates scheme operation when a low-voltage condition during the loss-of-field condition indicates that the system may collapse.
6. Dynamic simulation of loss-of-field and power-swing conditions is highly recommended for selecting and setting loss-of-field protection schemes. The simulation models should include the generator and its control systems, the step-up transformer, and the external power system. Generator models should include at least the turbine

speed governor, automatic voltage regulator, and power system stabilizer (PSS). These generator models should be validated using field test results.

7. Simulation results may be presented in an impedance plane together with the time dimension. This three-dimension resistance-reactance-time (R-X-t) space allows you to visualize the apparent impedance trajectory as time progresses. Make projections of the R-X-t representation on the R-t or the X-t planes to determine the instant at which relay elements start operation.
8. The impact of the loss-of-field condition on the generator and the power system depends mainly on the generator initial loading condition. In our simulations, we found that with an initial load of 150 MW, the generator loses synchronism as a result of the loss-of-field condition in all the cases. With an initial load of 40 MW, the generator, operating without excitation, remained in synchronism, working as a reluctance synchronous generator.
9. Insertion of a discharge resistor in the field circuit when the field breaker opens reduces the time constant of the exponentially decaying magnetic flux, thus accelerating the loss of synchronism.
10. When two generators are on line, the loss-of-field condition of one of them causes a lower voltage depression than when only one generator is on line. However, with two generators on line, the generator that loses excitation consumes more reactive power and has higher armature current because of the higher voltage.
11. Loss-of-synchronism simulation results show that using active-power blinders to restrict the width of the loss-of-field element characteristic along the real axis of the P-Q plane enhances scheme security for power swings.

## VII. APPENDIX A. POWER SYSTEM DATA

External Power System Data (Cases 1 Through 4)	
Positive-sequence equivalent impedance	9.4669 + j41.1368 ohms at 230 kV
Equivalent source (phase voltage)	134.5 kV
Generator Data	
Rated voltage	15 kV
Rated MVA	202 MVA
Rated active power (turbine)	160 MW
Poles	2
$X_d$	1.540 p.u.
$X_q$	1.520 p.u.
$X_d'$	0.170 p.u.
$X_q'$	0.246 p.u.
$X_d''$	0.123 p.u.
$X_q''$	0.123 p.u.
$T_{do}'$	9.1 s
$T_{do}''$	0.035 s

$T_{qo}''$	0.054 s
Total inertia constant (H)	3.18 kW-s/kVA
Step-Up Transformer Data	
Rated MVA	120/200 MVA
Rated voltage	15/230 kV
Z%	8.1% at 120 MVA
Connection	DY11
Governor	
Droop	5%
Field Circuit and Excitation System	
Nominal field voltage	280 Vdc
Nominal field current	1290 Adc
Field resistance	0.1947 $\Omega$
Field discharge resistance	0.2 $\Omega$
Control systems	See Fig. 43
Protection Scheme	
CTR	10000/5
VTR	15000/120
Loss-of-field relay settings	See Fig. 10

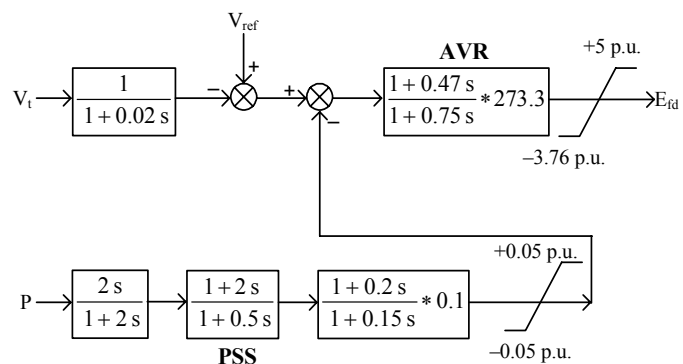


Fig. 43 Generator control-system block diagram

## VIII. APPENDIX B: METHODS TO DEFINE THE GENERATOR CAPABILITY CURVE, MEL, AND SSSL CHARACTERISTICS

Three methods to define these characteristics are:

1. Create a reference table with P and Q points, obtained from the characteristic, and perform a linear interpolation between adjacent points to approximate the actual curve. This gives a piecewise linear approximation.
2. Create a reference table with P and Q points, obtained from the characteristic, and use a curve-fitting algorithm to obtain the expressions (for example, quadratic equations) that approximate the different curves composing the capability curve.
3. Use circle equations to approximate the different curves composing the capability curve.

We can use each one of these methods to approximate the capability curve, MEL, and SSSL characteristics. Circle equations (Method 3) typically provide fairly accurate approxima-

tions of capability curves and SSSL characteristics; MEL characteristics may require a linear interpolation or a quadratic curve fitting. As an example, we discuss the application of Method 3 to define the capability curve.

Fig. 19 shows the capability curve and four points:  $(P_0, Q_0)$ ,  $(P_1, Q_1)$ ,  $(P_2, Q_2)$  and  $(P_3, Q_3)$ . With these points, we can determine the three circle equations to approximate the capability curve.

#### A. Armature-Current Heating Limit

The armature-current heating limit curve shown in Fig. 44 can be approximated with the following circle equation:

$$S(\beta) = R \cdot e^{i\beta} + i \cdot C \text{ for } -\alpha \leq \beta \leq \phi \quad (13)$$

Where  $R$  is the radius of the circle,  $C$  defines the position of the circle center ( $C = 0$  in this case),  $\phi$  is the circle upper limit that corresponds to the minimum lagging power factor ( $PF_{Lag}$ ), and  $-\alpha$  is the circle lower limit that corresponds to the minimum leading power factor ( $PF_{Lead}$ ).

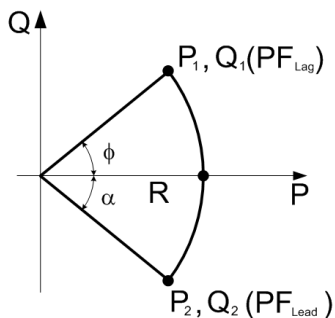


Fig. 44 Armature-current heating limit circle

We can determine  $R$ ,  $\phi$ , and  $\alpha$  from (14), (15), and (16):

$$R = S_{nom} \quad (14)$$

$$\phi = \cos^{-1} (PF_{Lag}) = \cos^{-1} (P_1 / S_{nom}) \quad (15)$$

$$\alpha = \cos^{-1} (PF_{Lead}) = \cos^{-1} (P_2 / S_{nom}) \quad (16)$$

Where  $PF_{Lag}$  is the minimum lagging power factor,  $PF_{Lead}$  is the minimum leading power factor, and  $S_{nom}$  is the generator nominal capacity.

#### B. Field-Current Heating Limit

The field-current heating limit curve shown in Fig. 45 can be approximated with the following circle equation:

$$S(\beta) = R \cdot e^{i\beta} + i \cdot C \text{ for } \rho \leq \beta \leq \frac{\pi}{2} \quad (17)$$

Where  $R$  is the radius of the circle,  $C$  defines the position of the circle center, and  $\rho$  is the circle lower limit.

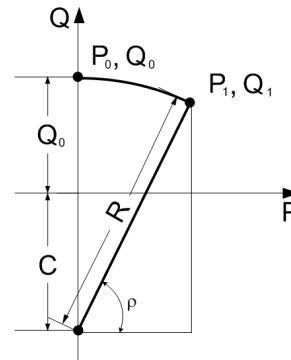


Fig. 45 Field-current heating limit circle

We need to solve (18), (19), and (20) to obtain  $R$ ,  $C$ , and  $\rho$ :

$$R \cdot \cos \rho = P_1 \quad (18)$$

$$R \cdot \sin \rho + C = Q_1 \quad (19)$$

$$R + C = Q_0 \quad (20)$$

#### C. Stator-End Core Heating Limit

The stator-end core heating limit curve shown in Fig. 46 can be approximated with the following circle equation:

$$S(\beta) = R \cdot e^{i\beta} + i \cdot C \text{ for } \frac{3}{2} \cdot \pi \leq \beta \leq -\gamma \quad (21)$$

Where  $R$  is the radius of the circle,  $C$  defines the position of the circle center, and  $-\gamma$  is the circle upper limit.

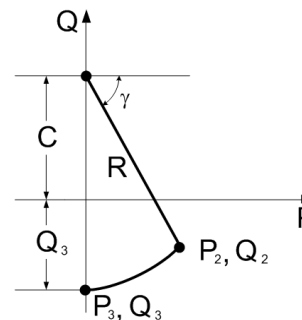


Fig. 46 Stator-end core heating limit circle

We need to solve (22), (23), and (24) to obtain  $R$ ,  $C$ , and  $\gamma$ .

$$R \cdot \cos \gamma = P_2 \quad (22)$$

$$C - R \cdot \sin \gamma = Q_2 \quad (23)$$

$$C - R = Q_3 \quad (24)$$

## IX. REFERENCES

- [1] D. Reimert, *Protective Relaying for Power Generation Systems*. Boca Raton: CRC Press, 2006.
- [2] P. Kundur, *Power System Stability and Control*. New York: McGraw-Hill, 1994.
- [3] S. B. Farnham and R. W. Swarthout, "Field excitation in relation to machine and system operation," *AIEE Trans.*, vol. 72, pt. III, no. 9, pp. 1215–1223, Dec. 1953.

- [4] S. S. Choy and X. M. Xia, "Under excitation limiter and its role in preventing excessive synchronous generator stator end-core heating," *IEEE Trans. Power Syst.*, vol. 15, no. 1, pp. 95–101, February 2000.
- [5] *Requirements for Cylindrical Rotor Synchronous Generators*, 1989. ANSI Std. C50.13–1989.
- [6] *Standard for Requirements for Salient-Pole Synchronous Generators and Generator/Motors for Hydraulic Turbine Applications*, 1982. ANSI Std. C50.12–1982.
- [7] J. L. Blackburn, *Protective Relaying, Principles and Applications*, 2nd Edition. New York-Basel: Marcel Dekker, Inc., 1998.
- [8] F. P. DeMello and C. Concordia, "Concepts of synchronous machine stability as affected by excitation control," *IEEE Trans. Power App. Syst.*, vol. PAS–88, No. 4, pp. 316–329, April 1969.
- [9] *IEEE Guide for AC Generator Protection*, 1995, IEEE Standard C37.102–1995.
- [10] *Draft Guide for AC Generator Protection*, IEEE Standard C37.102/D7–200X, April 2006.
- [11] C. K. Seetharaman, S. P. Verma, and A. M. El-Serafi, "Operation of synchronous generators in the asynchronous mode," *IEEE Trans. Power App. Syst.*, vol. PAS–93, pp. 928–939, 1974.
- [12] C. R. Mason, "A new loss of excitation relay for synchronous generators," *AIEE Trans.*, vol. 68, pt. II, pp. 1240–1245, 1949.
- [13] J. Berdy, "Loss-of excitation protection for modern synchronous generators," General Electric Co. Document GER-3183.
- [14] R. L. Tremaine and J. L. Blackburn, "Loss-of-field protection for synchronous machines," *AIEE Trans.*, vol. 73, pt. III, pp. 765–772, August 1954.
- [15] P. M. Anderson, *Power System Protection*. New York: IEEE Press/McGraw-Hill, 1999.
- [16] R. Sandoval, "The three dimensions of impedance: loss of field protection of a synchronous machine," *VIII Iberoamerican Symposium on Power System Protection*, Monterrey, N.L., Mexico, May 21–26, 2006 (in Spanish).
- [17] M. Stein, *Application Guide A03–0211*, ASEA Relays, December 1983.

## X. BIOGRAPHIES

**Ramón Sandoval** is a protection engineer for Comisión Federal de Electricidad at Topolobampo Thermal Power Station. He has worked for CFE since 1992 in electrical maintenance of power and industrial equipment such as induction motors, synchronous generators, breakers, AVRs, and step-up transformers. For the last five years he has been a power station protection engineer, installing, testing, and applying different types of protective equipment commonly used in industrial plants and power systems. This includes a variety of electromechanical, static and digital multifunction relays. He received training in power system modeling and simulation from LAPEM using ATP and has worked developing field procedures for protective relay testing using power system simulators and transient simulation software.

**Armando Guzmán** (M 1995, SM 2001) received his BSEE with honors from Guadalajara Autonomous University (UAG), Mexico, in 1979. He received a diploma in fiber-optics engineering from Monterrey Institute of Technology and Advanced Studies (ITESM), Mexico, in 1990, and his MSEE from University of Idaho, USA, in 2002. He served as regional supervisor of the Protection Department in the Western Transmission Region of the Federal Electricity Commission (the electrical utility company of Mexico) in Guadalajara, Mexico for 13 years. He lectured at UAG in power system protection. Since 1993 he has been with Schweitzer Engineering Laboratories in Pullman, Washington, where he is presently Research Engineering Manager. He holds several patents in power system protection and metering. He is a senior member of IEEE and has authored and coauthored several technical papers.

**Héctor J. Altuve** received his BSEE degree in 1969 from the Central University of Las Villas, Santa Clara, Cuba, and his Ph.D. in 1981 from Kiev Polytechnic Institute, Kiev, Ukraine. From 1969 until 1993, Dr. Altuve served on the faculty of the Electrical Engineering School, at the Central University of Las Villas. He served as professor, Graduate Doctoral Program, Mechanical and Electrical Engineering School, at the Autonomous University of Nuevo León, Monterrey, Mexico, from 1993 to 2000. In 1999–2000, he was the Schweitzer Visiting Professor at Washington State University's Department of Electrical Engineering. In January 2001, Dr. Altuve joined Schweitzer Engineering Laboratories, Inc., where he is currently a Distinguished Engineer and Director of Technology for Latin America. He has authored and coauthored more than 100 technical papers and holds three patents. His main research interests are in power system protection, control, and monitoring. Dr. Altuve is an IEEE Senior Member and a PES Distinguished Lecturer.